SIRT2- and NRF2-Targeting Thiazole-Containing Compound with Therapeutic Activity in Huntington's Disease Models

Quinti, Luisa; Casale, Malcolm; Moniot, Sébastien; Pais, Teresa F.; Van Kanegan, Michael J.; Kaltenbach, Linda S.

Published in:
Cell Chemical Biology

DOI:
10.1016/j.chembiol.2016.05.015

Publication date:
2016

Title: A novel structural scaffold of polypharmacological compounds with therapeutic activity in Huntington's disease models

Luisa Quinti [1,*], Malcolm Casale [2,*], Sébastien Moniot [3, *], Teresa F. Pais [4], Michael J. Van Kanegan [5], Linda S. Kaltenbach [5], Judit Pallos [6], Ryan G. Lim [7], Sharadha Dayalan Naidu [8], Heike Runne [9], Lisa Meisel [3], Nazifa Abdul Rauf [1], Dmitriy Leyfer [1], Michele M. Maxwell [1], Eddine Saiah [10], John E. Landers [11], Ruth Luthi-Carter [9], Ruben Abagyan [12], Albena T. Dinkova-Kostova [8, 13], Clemens Steegborn [3], J. Lawrence Marsh [7], Donald C. Lo [5], Leslie M. Thompson [2, 7, 14] and Aleksey G. Kazantsev [1,#]

* Author contributed equally

Corresponding author

Author's affiliation

1 Department of Neurology, Harvard Medical School and Massachusetts General Hospital, Boston, MA 02114
2 Department of Neurobiology and Behavior, University of California, Irvine, CA 92697
3 Department of Biochemistry, University of Bayreuth, 95447, Bayreuth, Germany
4 Cell and Molecular Neuroscience Unit, Instituto de Medicina Molecular, Av. Prof. Egas Moniz, 1649-028, Lisboa, Portugal
5 Center for Drug Discovery and Department of Neurobiology, Duke University Medical Center, Durham, NC 27710
6 Department of Developmental and Cell Biology, University of California, Irvine, CA 92697
7 Department of Biological Chemistry, University of California, Irvine, CA 92697
8 Division of Cancer Research, School of Medicine, University of Dundee, Dundee DD1 9SY, Scotland, United Kingdom
9 Functional Neurogenomics, Brain Mind Institute, Ecole Polytechnique Fédérale de Lausanne, 1015 Lausanne, Switzerland
10 BioTherapeutics Chemistry, Pfizer Worldwide Medicinal Chemistry, 200 Cambridge Park Drive, Cambridge, MA 02140, USA
11 Department of Neurology, University of Massachusetts Medical School, Worcester, MA, 01655
12 Skaggs School of Pharmacy and Pharmaceutical Sciences, University of California, San Diego, CA 92093-0747
13 Departments of Medicine and Pharmacology and Molecular Sciences, Johns Hopkins University School of Medicine, Baltimore, MD 21205
14 Department of Psychiatry and Human Behavior, University of California, Irvine, CA 92697

 # Corresponding Author: Aleksey Kazantsev: akazantsev@mgh.harvard.edu

Summary

There are currently no disease-modifying therapies for the neurodegenerative disorder Huntington's disease (HD). This study identified novel thiazole-containing inhibitors of the deacetylase sirtuin-2 (SIRT2) with neuroprotective activity in ex vivo brain slice and Drosophila models of HD. A systems biology approach revealed an additional SIRT2-independent property of the lead-compound, MIND4, as an inducer of cytoprotective NRF2 (nuclear factor-erythroid 2 p45-derived factor 2) activity. Structure-activity relationship studies further identified a potent NRF2 activator (MIND4-17) lacking SIRT2 inhibitory activity. MIND compounds induced NRF2 activation responses in neuronal and non-neuronal cells and reduced production of reactive oxygen species and nitrogen intermediates. These drug-like thiazole-containing compounds represent an exciting opportunity for development of multi-targeted agents with potentially synergistic therapeutic benefits in HD and related disorders.

Highlights

* Novel thiazole-containing inhibitors of sirtuin-2 deacetylase identified

* Lead-compound is neuroprotective in Huntington's disease models

* Lead-compound is SIRT2-independent inducer of NRF2-dependent responses

* Novel NRF2 inducers reduce levels of reactive oxygen and nitrogen species

Introduction

Mammalian NAD^+-dependent sirtuin deacetylases (SIRT1-SIRT7) regulate diverse physiological functions in cells and are implicated as potential modifiers of age-related human diseases (Donmez et al, 2013). The second family member, sirtuin-2 (SIRT2), was originally identified as α-tubulin deacetylase (North, et al, 2003). Later studies, however, indicated that SIRT2 deacetylates a broad variety of protein substrates and regulates multiple cellular processes, including histone remodeling and gene transcription (Taylor et al, 2008; Rauh et al, 2013). SIRT2 is a highly abundant protein in the adult CNS (Maxwell et al, 2011), including in neurons, although its precise function(s) remains uncertain (Maxwell et al, 2011; Luthi-Carter, 2010). We previously identified neuroprotective properties associated with several selective inhibitors of SIRT2 deacetylase (Chopra et al., 2012; Luthi-Carter et al., 2010; Outeiro et al., 2007).

Huntington's disease (HD), an autosomal dominant and progressive neurodegenerative disorder, is caused by expansion of a polymorphic trinucleotide repeat sequence $(CAG)_n$ within the gene encoding the large, highly conserved protein, Huntingtin (HTT) (1993). The expression of mutant HTT induces complex pathogenic mechanisms and alterations in multiple cellular pathways, including but not limited to protein folding and clearance, transcriptional dysregulation, and mitochondrial dysfunction. No single neurodegenerative mechanism has emerged as the predominant mechanism and this complex disease pathology challenges effective development of neurotherapies.

The harmful role of oxidative stress has been described in both HD patients and in experimental models (Browne and Beal, 2006; Sorolla et al.), and is potentially due to inherent sensitivity of neurons to an excess of reactive oxygen species (ROS) (Johri and Beal, 2012; Li et al., 2010; Stack et al., 2008; Tsunemi et al., 2012). Excessive oxidative stress has also been implicated in the pathology of other age-dependent neurodegenerative disorders with high

prevalence such as Alzheimer's and Parkinson's diseases (Moller, 2010; Quintanilla and Johnson, 2009; Zadori et al., 2012).

The initial goal of the present study was to identify a new scaffold(s) of potent and selective SIRT2 inhibitors and to assess the therapeutic potential of these compounds in models of neurodegenerative diseases (Chopra et al., 2012; Luthi-Carter et al., 2010; Outeiro et al., 2007; Pallos et al., 2008). We identified and characterized a novel structural scaffold MIND4, which transpired to contain compounds with dual SIRT2 inhibition and antioxidant NRF2 (nuclear factor-erythroid 2 p45-derived factor 2) activation properties.

Results

Identification of a lead series of novel SIRT2 inhibitors

To identify novel SIRT2 inhibitors, a scaffold-hopping approach was taken. We used derivatives of 8-nitro-5-R-quinoline and 5-nitro-8-R-quinoline, previously identified as substructures of bioactive compounds, as starting templates to create an initial focused library for screening compound activities in biochemical acetylation assays with human recombinant SIRT2 protein (Bodner et al., 2006; Outeiro et al., 2007). Compounds were screened at a single concentration (10 μM) in triplicate in biochemical SIRT2 assays and counter-screened against SIRT3 activity to assess target selectivity. Using iterative structure-activity chemical modifications to improve potency and selectivity, we identified compound 5-nitro-8-{[5-(phenoxymethyl)-4-phenyl-4H-1,2,4-triazol-3-yl]thio}quinoline, henceforth MIND4 (**Fig. 1A, B**). *In vitro* activity tests of MIND4 showed selective concentration-dependent inhibition of human recombinant SIRT2 deacetylase activity (**Fig. 1C-E**). A structure-activity relationship (SAR) study identified additional thiazole analogs with selective SIRT2 inhibition activity, however with lower potency than the parent compound MIND4 (**Fig.1G**). Intriguingly, a close structural analog 5-nitro-2-{[5-(phenoxymethyl)-4-phenyl-4H-1,2,4-triazol-3-yl]thio}pyridine,

henceforth MIND4-17 (**Fig.1G**), lacked any SIRT2 inhibition activity in the tested concentration range of 0.1-10 μM (**Fig. 1F**).

Characterization of a selective SIRT2 inhibition mechanism of the lead inhibitor MIND4

The precise potency of SIRT2 inhibition by MIND4 was determined as IC_{50}=1.2±0.2 μM in a concentration-dependent activity test with human recombinant SIRT2 deacetylase (**Fig. 2A**). A subsequent mechanistic study revealed competitive inhibition with NAD^+ and non-competitive inhibition with the peptide substrate with Ki of 2.1±0.2 μM (**Fig. 2B, C**). We used these results and molecular docking to generate a model of a SIRT2/MIND4 complex, which defines a molecular basis for compound selectivity against SIRT2 (**Fig. 2D**). The model shows partial MIND4 overlap with the NAD^+ binding site but not with the acetyl lysine site. Superimposition of the complex with SIRT1 and SIRT3 shows that MIND4 fits the larger SIRT2 active site. SIRT1 isoleucine-316 (Ile316) and SIRT3 leucine-395 (Leu395) and the corresponding helices would clash with MIND4, providing a rationale for SIRT2 selectivity.

Bioactivity of SIRT2 inhibitor MIND4

The activity of MIND4 was tested in rat embryonic striatal ST14A cells stably expressing a 546 amino acid HTT fragment containing either a wild-type (26Q) or expanded (128Q) polyglutamine repeat (Ehrlich et al., 2001; Quinti et al., 2010). Consistent with the properties of a SIRT2 deacetylase inhibitor, MIND4 treatment increased acetylation of α-tubulin lysine-40 (K40) in both wild-type and HD cells (**Fig. 3A, B, C**) (North et al., 2003). Next, MIND4 activity was examined in wild-type primary cortical neurons (DIV11), which preferentially express full-length SIRT2 (isoform SIRT2.1) and are enriched in the brain SIRT2.2 isoform (**Fig. 3E**) (Maxwell et al., 2011). Transient 6 h treatment with MIND4 did not increase acetylation of cytoplasmic α-tubulin (K40), but upregulated acetylation of known nuclear H3 histone substrates

lysine-56 and lysine-27; acetylation levels of lysine-14 of H3 histone were unchanged (Rauh et al., 2013), (**Fig. 3 E, F**). An increase in histone acetylation suggests that such SIRT2 inhibition could influence gene transcription as reported in previous work (Luthi-Carter et al., 2010).

Treatment with MIND4 is neuroprotective in HD models

Next, rat corticostriatal brain slice explants were used to test the neuroprotective potential of MIND4 in a complex neural tissue system expressing HTT exon 1 with expanded CAG repeats (mHTTex1) (Reinhart et al., 2011). Treatment with MIND4 significantly protected against mHTTex1-induced neurodegeneration in a concentration-dependent manner (**Fig. 3G**). Neuroprotection at the highest 10 μM concentration of MIND4 was comparable to the efficacy of a reference compound, the pan-caspase inhibitor Boc-D-FMK (C) at 100 μM (Varma et al., 2007). MIND4 was further tested in an additional *in vivo* setting using a *Drosophila* model of HD, in which neuroprotective effects of SIRT2 inhibition has been established in previous studies (Marsh et al., 2003; Pallos et al., 2008). In this model, degeneration of photoreceptor neurons is visually scored by the presence of surviving rhabdomeres in the eyes of *Drosophila* expressing mHTTex1 (Steffan et al., 2001). Flies treated with 10 μM MIND4 had significantly more surviving rhabdomeres than untreated controls (**Fig. 3H**). The neuroprotective effects of MIND4 were confirmed in an independent second trial conducted at the 10 μM dose (data not shown). Relative rescue was estimated as 22.6% and 20.7% for the first and second trials, respectively.

MIND4 induces transcriptional activation of the NRF2 pathway in HD and wild-type neuronal cells

Next we sought to determine whether MIND4 treatment could alter gene expression, possibly restoring or compensating for transcriptional dysregulation in HD models as a possible neuroprotective mechanism (Crook and Housman, 2011; Luthi-Carter et al., 2002; Luthi-Carter et al., 2010). We thus performed gene expression profiling to determine the impact of MIND4 on

transcriptional readouts in wild-type and HD ST14A cells.

Mutant HD and wild-type ST14A cells (Ehrlich et al., 2001; Quinti et al., 2010) were treated with MIND4 at 5 μM for 24 h. RNA from MIND4-treated and untreated HD mutant and wild-type ST14A cells was extracted and run on Affymetrix rat microarrays (Affy GeneChip Rat Genome 230 2.0 array) (http://www.ncbi.nlm.nih.gov/geo/query/acc.cgi?acc=GSE49392). Duplicates for each experimental condition were imported into Partek Genome Suite for biostatistical analysis. Genes showing significant differential expression were identified by ANOVA for three contrasts resulting in three gene-lists: mutant HD (MT) vs. wild-type (WT) = Case I (Disease Phenotype); MT/MIND4 treated vs. WT = Case II (Treatment Phenotype), and MT/MIND4 treated vs. MT = Case III (Mutant Drug-Dependent Phenotype) (**Table 1**). These represented transcriptional alterations in MT compared to WT cells (Case I), in MT treated compared to WT cells (Case II), and in MT treated cells compared to untreated MT cells (Case III). The lists, Cases I-III, were then imported into Ingenuity Pathway Analysis (IPA - Ingenuity Systems, www.ingenuity.com) for pathway and network analyses.

Surprisingly, in treated MT cells compared to untreated MT cells (Case III), all top seven of the most significant canonical pathways activated by MIND4 treatment were either directly or indirectly related to NRF2; in decreasing order of significance, these were: 1) the NRF2-mediated oxidative stress response itself, 2) glutathione-mediated detoxification, 3) LPS/IL-1 mediated inhibition of RXR function, 4) aryl hydrocarbon receptor signaling, 5) xenobiotic metabolism signaling, 6) glutathione redox reactions, and 7) glutathione biosynthesis (**Fig. 4A; p**lease see Discussion for more details). Fig. 4B shows a portion of the IPA canonical pathway of NRF2 colored by intensity correlated to fold-change of gene expression in treated versus untreated MT cells.

Next we tested whether MIND4 could also induce transcription of ARE genes in primary neurons. Wild-type rat primary striatal neurons were treated with MIND4 at a 5 μM dose for 24 h and subjected to transcriptional microarray analysis as described (Luthi-Carter et al., 2010). The

analysis of transcriptional changes shows that treatment with MIND4 induced a robust expression of canonical NRF2 gene targets in primary neurons as well (**Table S1**, **Supplemental Information)**.

These results suggested the intriguing possibility that MIND4 is an inducer of NRF2, acting through a SIRT2 inhibition-dependent or -independent mechanism.

MIND4 induces NRF2 activation response in SIRT2-independent manner

To validate the transcriptional microarray data, wild-type and mutant HD ST14A cells were treated with MIND4 for 24 h, and the expression levels of two canonical NRF2-responsive proteins, NQO1 and GCLM, were examined. Concentration-dependent increases in these proteins were observed in both cell lines, consistent with activation of NRF2 (**Fig. 5A**, **B**).

Next, we examined the effects of MIND4 on the stabilization of NRF2 protein, a well-known step in the cascade of pathway activation. The effects of MIND4 on NRF2 levels were compared with the reference NRF2-inducer sulforaphane (SFP) (Kensler et al., 2007; Lee et al., 2003; Zhang et al., 1992). Compounds were tested in COS1 cells transfected with plasmid constructs encoding NRF2-V5 proteins and β-galactosidase to normalize transfection efficiency between samples as described (McMahon et al., 2010). Treatment with both compounds resulted in stabilization of NRF2, as determined by the clear increases in protein levels (**Fig. 5C**). These results further support the finding that MIND4 is an inducer of the NRF2 pathway.

Treatment with the structural analog MIND4-11, also a SIRT2 inhibitor (IC_{50}=4 μM), had no effect on induction of the NRF2 response (**Fig. 5D**), further supporting a SIRT2-independent mechanism of NRF2 activation for MIND4. In contrast, treatment with the close structural analog MIND4-17, lacking SIRT2 inhibition activity, led to an even more potent induction of the NRF2-responsive proteins NQO1 and GCLM compared to MIND4 in both wild-type and HD mutant ST14A cells (**Fig. 5E, D**). Together, the findings suggest that the parent compound MIND4 is also an inducer of NRF2, activating this pathway via a SIRT2 inhibition-independent mechanism.

Thiazole analogs MIND4 and MIND4-17 induces NRF2 activation response in primary mouse neurons and astroglia

To extend evaluation of the NRF2 activation properties of MIND4 and MIND4-17 analogs, compound effects were tested in primary mouse neurons. A concentration-dependent induction of NQO1 and GCLM proteins in wild-type mouse cortical neurons (6 DIV) treated with MIND4-17 for 24 h supported a direct induction of the NRF2 pathway (**Fig. 6G**). These results showed that treatment with MIND4-17 can induce canonical NRF2 activation responses in mouse neurons.

Next, we examined whether MIND4-17 similarly to MIND4 could mediate transcriptional activation of canonical NRF2-responsive ARE genes. To that end we first used an ARE response element transcriptional reporter assay in a rat corticostriatal neuronal co-culture system (Kaltenbach et al., 2010). As shown in Fig. 5H, MIND4-17 significantly increased the transcriptional rate of a 5x-ARE-luciferase reporter construct transiently transfected into corticostriatal co-cultures. As would be expected for direct activation of NRF2, an almost saturating transcriptional response was already observed within 4 h of compound treatment.

Next, we determined whether MIND4-17 activates downstream ARE-dependent transcription of endogenous NRF2-target genes in native corticostriatal co-cultures. Treatment with MIND4-17 for 6 h significantly and concentration-dependently increased the expression of the canonical ARE genes *Nqo1*, *Hmox1*, *Srx1*, and to a lesser degree *Gclc* (**Fig. 5I-L).** These same genes were activated in primary rat neuronal cultures by MIND4 (**Table S1**). Finally, we compared the effects of MIND4 and MIND4-17 on transcriptional activation of NRF2 pathway in the context of the HD mutation. Both compounds showed similar concentration-dependent activation of the 5x-ARE-luciferase reporter in corticostriatal co-cultures derived from wild-type vs. an HD mutant knock-in mouse model (Q175/+) (Menalled et al., 2012). Treatment of cultures with MIND4-17 for 24 h was not significantly cytotoxic for striatal (5 DIV) or cortical (5 DIV)

neurons, differentially labeled in co-culture (**Fig. S1**).

To extend the validation of NRF2 activation properties in non-neuronal cells, we tested MIND4 and MIND4-17 in primary mouse astroglia. Treatment with both compounds resulted in concentration-dependent increases of NRF2-responsive NQO1 and GCLM protein levels, demonstrating that effects of these inducers are not restricted to neuronal cells (**Fig. 5O, P**).

NRF2 inducer MIND4 and its structural analog MIN4-17 reduce ROS levels in microglia

We next performed functional studies evaluating properties of MIND4 and MIND4-17 in a well-characterized microglia model of NRF2 activation (Innamorato et al., 2008; Koh et al., 2011) using lentiviral transduction of SIRT2 shRNA or a scrambled control (**Fig. 6A)**. The effects of both compounds on the levels of reactive oxygen species (ROS) were examined in microglia activated with LPS/TNFα as described (Pais et al., 2013). Treatment with MIND4 or MIND4-17 resulted in a decrease of ROS levels in wild-type microglia (**Fig. 6B**), Notably, the effect of MIND4-17 was more pronounced than the effect of MIND4 and in agreement with the difference in inducer potencies of NRF2 activation. SIRT2 knockdown in microglia caused a significant elevation of ROS levels as previously described (**Fig. 6 B, C**) (Pais et al., 2013). Nonetheless, treatment with MIND4-17 was still able to decrease ROS levels, albeit with lower magnitude than in wild-type microglia (**Fig. 6C**). The effects of MIND4 treatment on ROS levels were undetectable and likely due to its lower potency of NRF2 activation.

Since SIRT2 knockdown led to an increase, not a decrease, in ROS levels in microglia (Pais et al., 2013), SIRT2 inhibitory activity of MIND4 is presumably irrelevant for the observed antioxidant effects of MIND4 in wild-type microglia. Moreover, the antioxidant effects of MIND4-17 in wild-type and SIRT2-null microglia are clearly independent from SIRT2 since this compound lacks SIRT2 inhibitory activity. Together, these findings indicate that the antioxidant effects of both MIND4 and MIND4-17 are attributable to the NRF2-activating properties of these compounds.

NRF2 inducers MIND4 and MIND4-17 reduce levels of reactive nitrogen intermediates (RNI) in microglia

Finally, to determine whether NRF2 activation through a SIRT2-independent mechanism could be observed in activated microglia, the effects of MIND4 and MIND4-17 on neurotoxic nitric oxide, produced by microglial iNOS, were examined (Aguilera et al., 2007; Reynolds et al., 2008; Tieu et al., 2003). Treatment with MIND4 and MIND4-17 reduced production of nitric oxide in a concentration-dependent manner in activated microglia, where the effect of MIND4-17 was again more pronounced (**Fig. 6 D**). The reduction of nitric oxide levels was similar in control cell (white bars) vs. those transduced with SIRT2 shRNA (black bars), and irrespective of the presence or absence of SIRT2 inhibitory activity in MIND4 vs. MIND4-17, respectively. These results were again consistent with a SIRT2-independent mechanism for NRF2 activationn, here resulting in the reduction of nitric oxide levels in activated microglia.

Discussion

We have identified a novel scaffold of thiazole-containing compounds which exhibits selective SIRT2- inhibition activity at various potencies. Mechanistic studies with the most potent compound elucidated an NAD^+-competitive mechanism of SIRT2 inhibition. MIND4 acts as a bioactive SIRT2 inhibitor, and is neuroprotective in *ex vivo* brain slice and *in vivo Drosophila* models of HD. Through a systems biology approach, we unexpectedly found that MIND4 is also a transcriptional inducer of the NRF2-mediated oxidative stress response and modulates multiple pathways (see Fig. 4A) all centrally regulated byNRF2 activation: in glutathione-mediated detoxification, NRF2 regulates the expression of multiple members of the glutathione transferase (GST) supergene superfamily, the enzymes that catalyse the conjugation of numerous xenobiotics with glutathione (Hayes and Dinkova-Kostova, 2014; Wu et al., 2012). In LPS/IL-1 mediated inhibition of RXR function, NRF2 binds directly to RXR through its Neh7 domain (Chorley et

al., 2012; Wang et al., 2013). In aryl hydrocarbon receptor signaling, NRF2 is often required for induction of classical AhR battery genes, e.g. by dioxin (Yeager et al., 2009). In xenobiotic metabolism signaling, NRF2 regulates genes encoding multiple drug-metabolizing enzymes (Pratt-Hyatt et al., 2013; Wu et al., 2012). In glutathione redox reactions, NRF2 regulates the enzymes that are responsible for regenerating and keeping glutathione in its reduced state (Hayes and Dinkova-Kostova, 2014). Finally, in glutathione biosynthesis, NRF2 regulates the expression of both subunits of the enzyme that catalyzes the rate-limiting step in glutathione biosynthesis (Moinova and Mulcahy, 1999). Moreover, MIND4 effects on gene transcription were confirmed to be translated into increased expression of NRF2-responsive proteins in both HD mutant and wild-type cells. Together, these results strongly implicate NRF2 as a central target of MIND4 activation.

The follow-up experiments with a close structural analog of MIND4, MIND4-17, suggested that the mechanism of NRF2 activation is SIRT2-independent. This conclusion was supported by results demonstrating similar effects of MIND4 and the known inducer SFP (Zhang et al., 1992) on stabilization of NRF2 protein, a well-defined step in the pathway activation by NRF2 inducers. A functional study showed that MIND4 and MIND4-17, the latter lacking detectable SIRT2 inhibition activity, both reduce production of ROS and RNI in microglia, consistent with the properties of NRF2 inducers. Together, these findings suggest that MIND4 and MIND4-17 represent a novel class of NRF2 activators.

The molecular mechanism of NRF2 activation was elucidated as targeting cytoplasmic KEAP1 adapter protein through covalent modification of major sensor-cysteine C151. That modification is resulted in conformational change and arrest of NRF2/KAEP1 complex, unable to target NRF2 for proteasome degradation, which leads to accumulation and nuclear translocation of *de novo* synthesized NRF2, and subsequent activation of ARE gene transcription. This NRF2 activation mechanism is described in depth in an accompanying manuscript.

Antioxidant activities mediated by the transcription factor NRF2 have emerged as a

potential therapeutic approach to combat neurodegeneration and aging (Johnson et al., 2008; Joshi and Johnson, 2012; Lee et al., 2003; Lewis et al., 2012; Petri et al., 2012; Stepkowski and Kruszewski, 2011; Tufekci et al., 2011; van Muiswinkel and Kuiperij, 2005; Xiong et al., 2015). Overexpression of NRF2 provides protection for primary neurons from expression of mutant HTT fragment (Tsvetkov et al., 2013), and the efficacy of pharmacological activation of NRF2 has been shown in HD mice and is associated with induction of broad antioxidant effects in brain (Ellrichmann et al., 2011; Stack et al., 2010).

Therefore, the discovery of a novel drug-like scaffold of thiazole-containing compounds as described here presents an opportunity to develop clinical lead candidates with distinct as well as combined/synergistic mechanisms of SIRT2 inhibition and/or NRF2 activation.

Experimental Procedures

Compound source and storage

Compounds were procured from ChemBridge Corp. San Diego (purity QC ensured by provided NMR), dissolved in molecular biology grade dimethyl sulfoxide (DMSO) to 10 mM stock concentration, aliquoted, and stored at -80 °C. Dimethyl fumarate was purchased from Sigma, dissolved to a 10 mM concentration in 100% DMSO, aliquoted and stored at -80 °C.

MIND4-17 has also been re-synthesized (purity >95%) and has shown essentially identical potency of NRF2 activation as compound in multiple batches purchased from Chembridge.

Characterization of compound-dependent inhibition of SIRT2 deacetylase activity

Modulation of sirtuin activity by compounds was assessed using the Fluor de Lys fluorescent biochemical assay (BioMol International, LP) in a 96-well format as described (Outeiro et al., 2007). Deacetylation reaction was performed at 37 ^{0}C for 1 h in the presence of human recombinant enzymes: SIRT1 (BioMol-SE-239) 1 unit/per reaction, SIRT2 (BioMol-SE-251) 5 units/per reaction, or SIRT3 (BioMol-SE-270) 5 units/per reaction, compound of interest,

standard buffer, 50 μM substrate, and 500 μM NAD^+ according to the manufacturer's protocol.

For analyzing the SIRT2 inhibition mechanism of MIND4 in a continuous coupled enzymatic assay with an α-tubulin peptide substrate, the recombinant enzyme was prepared and its activity analyzed as described previously (Moniot et al., 2013). The IC_{50} for MIND4 was determined using α-tubulin and NAD^+ at 150 μM and 500 μM, respectively. The titration with NAD^+ was performed at 150 μM α-tubulin peptide, and the peptide titration at 1 mM NAD^+. Data analysis and fitting was done in Grafit 7 (Erithacus Software, Horley, UK).

Docking model for selective binding of MIND4 to SIRT2

For generating the SIRT2/MIND4 complex model, the compound was docked using the program FlexX of the LeadIT suite (BioSolveIT, Germany) and a SIRT2/ADP-ribose structure (PDB ID 3ZGV) (Moniot et al., 2013); ligand omitted for the calculation) as the receptor. The MIND4 molecule, generated as a 3D SDF file in MarvinSketch (ChemAxon, Budapest, Hungary), was docked with FlexX using default parameters, i.e., hybrid enthalpy and entropy driven ligand binding, hard penalty on protein ligand clashes (maximum allowed overlap volume 3.2 $Å^3$), and average penalty on intra-ligand clashes (clash factor 0.6). The best pose was exported and visualized in Pymol (Schrödinger LLC, Portland, USA). The overlay with SIRT1 (PDB ID 4KXQ) and with SIRT3 in complex with carba-NAD and acetylated peptide (PDB ID 4FVT) was generated using the build-in align command of Pymol.

NRF2 stabilization assay

COS1 cells were plated 16 h before transfection. Cells were co-transfected with plasmids encoding wild-type KEAP1 and NRF2-V5 (generous gifts from Dr. M. MacMahon and Dr. John D. Hayes, University of Dundee) at 1:1 ratio. A plasmid encoding β-galactosidase was transfected as well to monitor transfection efficiency. 24 h post-transfection cells were exposed to MIND4 or sulforaphane for 3 h, harvested, lysed, and extracts were prepared and loaded on SDS-PAGE

normalized to β-gal expression activity. Samples were resolved on SDS PAGE and immunoblotted with V-5 antibody.

Rat embryonic striatal ST14A cells

Compound bioactivity was tested in the rat embryonic striatal cell lines ST14A, which stably express either a mutant expanded repeat (128Q) or wild-type (26Q) 546 amino acid huntingtin (HTT) fragment (generous gift of E. Cattaneo) (Ehrlich et al., 2001). ST14A cells were propagated at 33 °C in the presence of serum. To induce neuronal differentiation cells were serum deprived and cultured at 37 °C in presence of N2 supplement (Invitrogen). Cells were treated with compounds concurrently with induction of neuronal differentiation for 24 h, unless stated otherwise, as described (Quinti et al., 2010).

Protein extraction and Western analysis

To assess protein levels, cell extracts were prepared, washed with PBS and lysed with buffer containing 2% SDS, Complete EDTA-free Protease Inhibitor Cocktail (Roche) and 1 mM phenylmethylsulfonyl fluoride (Sigma). Protein concentrations in cell extracts were evaluated using a BCA analysis kit (Pierce 23225) and normalized. Samples were prepared in a SDS buffer containing DTT (New England Biolabs B7703S) and separated on bis-acrylamide protein gels via electrophoresis and transferred onto a 0.2 μm PVDF membrane (Bio-Rad 162-0177). Membranes were probed for NQO1 (Sigma N5288, 1:1,000), GCLM (Abcam ab126704, 1:800), SIRT2 (Sigma S8447, 1:2,500), histone H3 (Cell Signaling 4499, 1:2,000), acetylated H3 (K56) (Millipore 04-1135, 1:500), acetylated H3 (K27) (Cell Signaling 4353, 1:800), acetylated H3 (K9,K14) (Millipore 06-599, 1:10,000), GADPH (Millipore MAB374, 1:10,000), actin (Sigma A2066, 1:1250), α-tubulin (Sigma T6074, 1:10,000), and acetylated α-tubulin (Sigma T6793, 1:2,500). Membranes were thrice washed in PBST for 15 min on a shaker and incubated in either

an anti-rabbit-HRP (Bio-Rad 170-5046, 1:10,000) or anti-mouse-HRP (Sigma A3682, 1:4,000) secondary solution as appropriate in 3% milk in PBST for 1 h at room temperature on a rocker. After four washes of 15 min each in PBST on a shaker, blots were visualized using SuperSignal West Pico Chemiluminescent Substrate (Pierce 34080) or SuperSignal West Dura Extended Duration Substrate (Thermo 34075) and exposed on Scientific Imaging Film (Kodak 864 6770). Densitometric analyses of the Western blots were conducted using ImageJ software available from the National Institutes of Health, USA. Blot intensities for proteins of interest were normalized to GADPH or α-tubulin levels. Statistical analyses were performed using a Student's *t*-test.

Microarray data analysis

RNA was extracted from HD mutant and wild-type ST14A cells, differentiated for 24 h and treated with vehicle (DMSO) or with 5 μM MIND4, using the RNeasy kit (Qiagen). Labeled cRNAs were prepared and hybridized to Affymetrix GeneChip Rat Genome 230 2.0 microarrays according to the manufacturer's instructions. Affymetrix CEL (intensity) files from hybridized arrays were imported into the Partek Genome Suite, Partek Incorporated, for biostatistical analysis. 2 CEL files were used for each experimental condition: wild-type (WT) untreated, MIND4 treated (WT/MIND4), mutant (MTT) untreated, and mutant (MTT) MIND4-terated (MTT/MIND4). Two-way ANOVA was performed with interaction term included and evaluated three contrasts of interest (Case I, II, and III). Gene lists were created for each of the three contrasts using the thresholds of absolute value of fold-change > 1.5 and p-value with False Discovery Rate (FDR) < 0.05. The lengths of the gene lists are for Case I (DP)-1765 genes, for Case II (TP)-1797 genes, and for Case III (MDDP)-268 genes. These three gene lists were imported into Ingenuity IPA for pathway and network analyses. These analyses provided Networks (graph structures of molecules connected by relationships in the IPA knowledgebase), Functions (lists of molecules grouped together due to their contribution to a biological function)

and Canonical Pathways (molecules and relationships that participate in a biological pathway). Scores are assigned according to the probability that the genes from the user's list might appear in the function or pathway by chance (right-tailed Fisher's Exact Test).

Compound tests in acutely transfected rat brain slice culture assay

Coronal brain slices (250 μm thick) containing both cortex and striatum were prepared from CD Sprague-Dawley rat pups (Charles River) at postnatal day 10 and placed into interface culture as previously described (Reinhart et al., 2011). All experimental procedures including the sacrificing of animals were done in accordance with NIH guidelines and under Duke IACUC approval and oversight. A biolistic device (Helios Gene Gun; Bio-Rad) was then used to co-transfect the brain slices with YFP visual reporter and a mutant huntingtin plasmid containing human HTT exon-1 harboring a 73 CAG repeat to induce neurodegeneration of medium spiny neurons (MSNs). MIND4 was added to cultures wells at the time of slice preparation and transfection to a final DMSO concentration of 0.1%; this concentration of DMSO was also added to all control wells. The positive control used for these experiments was the pan-caspase inhibitor Boc-D-FMK (Sigma-Aldrich, Inc.) at 100 μM (Varma et al., 2007). YFP co-transfected MSNs were identified 4 days after incubation by their location within the striatum and by their characteristic dendritic arborization as previously described (Crittenden et al., 2010; Reinhart et al., 2011). Briefly, MSNs exhibiting normal-sized cell bodies, even and continuous expression of YFP within all cell compartments, and >2 discernable primary dendrites >2 cell bodies long were scored as healthy. Ordinate axis expresses the mean numbers of healthy YFP-positive MSNs per striatal region in each brain slice. Statistical significance was tested using ANOVA followed by Dunnett's *post hoc* comparison test at the 0.05 confidence level.

Transcriptional assays in primary corticostriatal neuronal co-cultures

Primary corticostriatal neuronal co-cultures were prepared from E18 WT or Q175/+ (Menalled et

al., 2012) mouse brains as previously described (Kaltenbach et al., 2010). All experimental procedures including the husbandry and sacrificing of animals were done in accordance with NIH guidelines and under Duke IACUC approval and oversight. For 5x-ARE-luciferase reporter assays, neurons were transfected following their isolation (Nucleofector, Lonza) with 2.5 μg Cignal Antioxidant Response Reporter dual luciferase plasmids (Qiagen/SABiosciences) and plated onto pre-established glial beds in 96 well plates. After 4 days in culture at 37 °C under 5% CO_2, co-cultures were treated with the indicated compounds for 4 h or 16 h then harvested and read for luminescence from firefly and *Renilla* luciferases according to the Dual Glo luciferase protocol (Promega) using a SpectraMaxL luminometer (Molecular Devices). Each sample was measured in technical triplicate. For quantitative RT-PCR (qPCR) of ARE target genes, corticostriatal co-cultures were prepared as described above and, after 4 days in culture, treated for 6 h with the indicated compounds followed by RNA harvesting according to the Absolutely RNA miniprep protocol (Agilent Technologies). Purified RNA was converted to cDNA using random hexamers and SuperScript First-Strand RT-PCR Synthesis (Invitrogen). Resulting cDNA samples were used for qPCR using Power SYBR Green (Applied Biosystems) and the ViiA 7 qPCR System (Applied Biosystems). C_t values were determined using primer sets against ARE genes *Hmox1*, *Srx, Gclc* and *Nqo1* (Yang et al., 2012). Each sample was run in technical triplicate and relative expression expressed as fold-change over control after normalizing each sample to C_t values for GAPDH.

Compound tests in a* Drosophila *model of HD

Treatment of a *Drosophila* HD model with compound and efficacy analysis of the effects of MIND4 on photoreceptor neurons was performed as described (Pallos et al., 2008). The indicated numbers of flies were scored for each condition (n) with the number of ommatidia scored indicated in parentheses. Trial 1: DMSO=11(449); MIND4 1 μM=3(112); MIND4 10 μM=9(337); MIND4 30 μM=9(364). Trial 2: DMSO=8(361); MIND4 10 μM=8(292). Relative

rescue of photoreceptor neurons in flies treated vs. untreated with MIND4 at 10 μM dose was estimated for Trial 1 and Trial 2 as 22.6% and 20.7%; t-test significance for Trial 1 was $p < 0.001$ and for Trial 2 was $p < 0.02$.

Compound tests using ROS/RNI assays in stimulated microglia cells

N9 microglial cells lentiviral-transduced with shRNA for SIRT2 knock-down or with a scrambled control shRNA were cultured in RPMI medium containing Glutamax (Invitrogen) and supplemented with 10% FBS (endotoxin levels lower than 10 EU/ml). Cells were plated in 96-well plates ($5x10^4$/well) and cultured overnight before stimulation with LPS (100 ng/ml) and TNF (10 ng/ml) for 20 h in medium supplemented with DMSO or with the tested compounds. ROS levels were detected by flow cytometry after microglia incubation with 10 μM 5-(and-6)-chloromethyl-2',7'-dichlorodihydrofluorescein diacetate, acetyl ester (CM-H_2DCFDA) (Invitrogen) for 20 min. The production of NO by iNOS was measured indirectly by assaying nitrites in the culture supernatant using the Griess reaction. Briefly, 100 μl of supernatants was incubated with an equal amount of Griess reagent (1% sulphanilamide, 0.1% naphthylethylenediamine in 2% phosphoric acid solution) and the absorbance read at 550 nm after 20 min of incubation at room temperature.

Author Contributions.

L.Q. conducted identification, characterization, and analysis of compound properties *in vitro*, was involved in manuscript preparation; D.L. and N.A.R. assisted with in vitro experiments; M.M.M. supervised compound characterization studies in primary neurons and assisted with manuscript preparation; M.C. performed IPA and identified NRF2 induction as a predominant activity of MIND4, R.G.L. assisted with gene expression analysis; J.E.L. performed the microarray and assisted with analysis; H.R. and R.L.C. performed independent gene transcription

study and microarray analysis; A.D.K. and S.D.N, planned and performed the experiments in NRF2 stabilization, A.D.K. participated in writing and editing of manuscript; T.F.P. tested compound effects on ROS/RNI in microglia; M.J.V.K. performed compound NRF2 transcriptional profiling in primary neuronal culture, L.S.K. tested MIND4 in brain slices; D. C. L. supervised the experiments, analyzed data, and edited the manuscript; J.P and J.L.M. were involved in the *Drosophila* studies; J.L.M. edited the manuscript; S.M., C.S. characterized compound SIRT2 inhibition activity, assisted by L.M.; C.S. edited manuscript; E.S. analyzed compound structures and provided chemistry expertise; R.B. performed the docking and modeling studies; L.M.T. was involved in planning transcriptional studies, data analysis, manuscript preparation; A.G.K. planned, organized, was involved in data mining and analysis, manuscript writing and preparation.

L.Q., M.C., and S.M. contribute equally to the work.

Acknowledgements

This work was supported by grants from the NIH U01-NS066912, R01NS04528, NIH NS078370, NIH NS080514, and NIGMS grant GM080356, the Biotechnology and Biological Sciences Research Council (BB/J007498/1, BB/L01923X/1), Alzheimer Forschung Initiative (grant 14834 to C.S.) and Cancer Research UK (C20953/A18644). We also acknowledge support from RJG foundation to L.Q and A.G.K and from the American Heart Association to R.G.L. This work was made possible in part by the availability of the Optical Biology Shared Resource of the Cancer Center Support Grant (CA-62203) at the University of California, Irvine. We thank Michael McMahon (University of Dundee) for plasmids encoding wild-type Keap1.

Authors declare no conflict of interest

References

(1993). A novel gene containing a trinucleotide repeat that is expanded and unstable on Huntington's disease chromosomes. The Huntington's Disease Collaborative Research Group. Cell *72*, 971-983.

Aguilera, P., Chanez-Cardenas, M.E., Floriano-Sanchez, E., Barrera, D., Santamaria, A., Sanchez-Gonzalez, D.J., Perez-Severiano, F., Pedraza-Chaverri, J., and Jimenez, P.D. (2007). Time-related changes in constitutive and inducible nitric oxide synthases in the rat striatum in a model of Huntington's disease. Neurotoxicology *28*, 1200-1207.

Bodner, R.A., Outeiro, T.F., Altmann, S., Maxwell, M.M., Cho, S.H., Hyman, B.T., McLean, P.J., Young, A.B., Housman, D.E., and Kazantsev, A.G. (2006). Pharmacological promotion of inclusion formation: a therapeutic approach for Huntington's and Parkinson's diseases. Proceedings of the National Academy of Sciences of the United States of America *103*, 4246-4251.

Browne, S.E., and Beal, M.F. (2006). Oxidative damage in Huntington's disease pathogenesis. Antioxid Redox Signal *8*, 2061-2073.

Chopra, V., Quinti, L., Kim, J., Vollor, L., Narayanan, K.L., Edgerly, C., Cipicchio, P.M., Lauver, M.A., Choi, S.H., Silverman, R.B.*, et al.* (2012). The Sirtuin 2 Inhibitor AK-7 Is Neuroprotective in Huntington's Disease Mouse Models. Cell reports *2*, 1492-1497.

Chorley, B.N., Campbell, M.R., Wang, X., Karaca, M., Sambandan, D., Bangura, F., Xue, P., Pi, J., Kleeberger, S.R., and Bell, D.A. (2012). Identification of novel NRF2-regulated genes by ChIP-Seq: influence on retinoid X receptor alpha. Nucleic acids research *40*, 7416-7429.

Crittenden, J.R., Dunn, D.E., Merali, F.I., Woodman, B., Yim, M., Borkowska, A.E., Frosch, M.P., Bates, G.P., Housman, D.E., Lo, D.C.*, et al.* (2010). CalDAG-GEFI down-regulation in the striatum as a neuroprotective change in Huntington's disease. Human molecular genetics *19*, 1756-1765.

Crook, Z.R., and Housman, D. (2011). Huntington's disease: can mice lead the way to treatment? Neuron *69*, 423-435.

Ehrlich, M.E., Conti, L., Toselli, M., Taglietti, L., Fiorillo, E., Taglietti, V., Ivkovic, S., Guinea, B., Tranberg, A., Sipione, S.*, et al.* (2001). ST14A cells have properties of a medium-size spiny neuron. Exp Neurol *167*, 215-226.

Ellrichmann, G., Petrasch-Parwez, E., Lee, D.H., Reick, C., Arning, L., Saft, C., Gold, R., and Linker, R.A. (2011). Efficacy of fumaric acid esters in the R6/2 and YAC128 models of Huntington's disease. PloS one *6*, e16172.

Hayes, J.D., and Dinkova-Kostova, A.T. (2014). The Nrf2 regulatory network provides an interface between redox and intermediary metabolism. Trends in biochemical sciences *39*, 199-218.

Innamorato, N.G., Rojo, A.I., Garcia-Yague, A.J., Yamamoto, M., de Ceballos, M.L., and Cuadrado, A. (2008). The transcription factor Nrf2 is a therapeutic target against brain inflammation. J Immunol *181*, 680-689.

Johnson, J.A., Johnson, D.A., Kraft, A.D., Calkins, M.J., Jakel, R.J., Vargas, M.R., and Chen, P.C. (2008). The Nrf2-ARE pathway: an indicator and modulator of oxidative stress in neurodegeneration. Annals of the New York Academy of Sciences *1147*, 61-69.

Johri, A., and Beal, M.F. (2012). Antioxidants in Huntington's disease. Biochimica et biophysica acta *1822*, 664-674.

Joshi, G., and Johnson, J.A. (2012). The Nrf2-ARE Pathway: A Valuable Therapeutic Target for the Treatment of Neurodegenerative Diseases. Recent patents on CNS drug discovery.

Kaltenbach, L.S., Bolton, M.M., Shah, B., Kanju, P.M., Lewis, G.M., Turmel, G.J., Whaley, J.C., Trask, O.J., Jr., and Lo, D.C. (2010). Composite primary neuronal high-content screening assay for Huntington's disease incorporating non-cell-autonomous interactions. J Biomol Screen *15*, 806-819.

Kensler, T.W., Wakabayashi, N., and Biswal, S. (2007). Cell survival responses to environmental stresses via the Keap1-Nrf2-ARE pathway. Annual review of pharmacology and toxicology *47*, 89-116.

Koh, K., Kim, J., Jang, Y.J., Yoon, K., Cha, Y., Lee, H.J., and Kim, J. (2011). Transcription factor Nrf2 suppresses LPS-induced hyperactivation of BV-2 microglial cells. Journal of neuroimmunology *233*, 160-167.

Lee, J.M., Calkins, M.J., Chan, K., Kan, Y.W., and Johnson, J.A. (2003). Identification of the NF-E2-related factor-2-dependent genes conferring protection against oxidative stress in primary cortical astrocytes using oligonucleotide microarray analysis. The Journal of biological chemistry *278*, 12029-12038.

Lewis, C.A., Manning, J., Rossi, F., and Krieger, C. (2012). The Neuroinflammatory Response in ALS: The Roles of Microglia and T Cells. Neurology research international *2012*, 803701.

Li, X., Valencia, A., Sapp, E., Masso, N., Alexander, J., Reeves, P., Kegel, K.B., Aronin, N., and Difiglia, M. (2010). Aberrant Rab11-dependent trafficking of the neuronal glutamate transporter EAAC1 causes oxidative stress and cell death in Huntington's disease. J Neurosci *30*, 4552-4561.

Luthi-Carter, R., Hanson, S.A., Strand, A.D., Bergstrom, D.A., Chun, W., Peters, N.L., Woods, A.M., Chan, E.Y., Kooperberg, C., Krainc, D.*, et al.* (2002). Dysregulation of gene expression in the R6/2 model of polyglutamine disease: parallel changes in muscle and brain. Human molecular genetics *11*, 1911-1926.

Luthi-Carter, R., Taylor, D.M., Pallos, J., Lambert, E., Amore, A., Parker, A., Moffitt, H., Smith, D.L., Runne, H., Gokce, O.*, et al.* (2010). SIRT2 inhibition achieves neuroprotection by decreasing sterol biosynthesis. Proceedings of the National Academy of Sciences of the United States of America *107*, 7927-7932.

Marsh, J.L., Pallos, J., and Thompson, L.M. (2003). Fly models of Huntington's disease. Human molecular genetics *12 Spec No 2*, R187-193.

Maxwell, M.M., Tomkinson, E.M., Nobles, J., Wizeman, J.W., Amore, A.M., Quinti, L., Chopra, V., Hersch, S.M., and Kazantsev, A.G. (2011). The Sirtuin 2 microtubule deacetylase is an abundant neuronal protein that accumulates in the aging CNS. Human molecular genetics *20*, 3986-3996.

McMahon, M., Lamont, D.J., Beattie, K.A., and Hayes, J.D. (2010). Keap1 perceives stress via three sensors for the endogenous signaling molecules nitric oxide, zinc, and alkenals. Proceedings of the National Academy of Sciences of the United States of America *107*, 18838-18843.

Menalled, L.B., Kudwa, A.E., Miller, S., Fitzpatrick, J., Watson-Johnson, J., Keating, N., Ruiz, M., Mushlin, R., Alosio, W., McConnell, K.*, et al.* (2012). Comprehensive behavioral and molecular characterization of a new knock-in mouse model of Huntington's disease: zQ175. PloS one *7*, e49838.

Moinova, H.R., and Mulcahy, R.T. (1999). Up-regulation of the human gamma-glutamylcysteine synthetase regulatory subunit gene involves binding of Nrf-2 to an electrophile responsive element. Biochemical and biophysical research communications *261*, 661-668.

Moller, T. (2010). Neuroinflammation in Huntington's disease. J Neural Transm *117*, 1001-1008.

Moniot, S., Schutkowski, M., and Steegborn, C. (2013). Crystal structure analysis of human Sirt2 and its ADP-ribose complex. Journal of structural biology *182*, 136-143.

North, B.J., Marshall, B.L., Borra, M.T., Denu, J.M., and Verdin, E. (2003). The human Sir2 ortholog, SIRT2, is an NAD+-dependent tubulin deacetylase. Molecular cell *11*, 437-444.

Outeiro, T.F., Kontopoulos, E., Altmann, S.M., Kufareva, I., Strathearn, K.E., Amore, A.M., Volk, C.B., Maxwell, M.M., Rochet, J.C., McLean, P.J.*, et al.* (2007). Sirtuin 2 inhibitors rescue alpha-synuclein-mediated toxicity in models of Parkinson's disease. Science *317*, 516-519.

Pais, T.F., Szego, E.M., Marques, O., Miller-Fleming, L., Antas, P., Guerreiro, P., de Oliveira, R.M., Kasapoglu, B., and Outeiro, T.F. (2013). The NAD-dependent deacetylase sirtuin 2 is a suppressor of microglial activation and brain inflammation. The EMBO journal *32*, 2603-2616.

Pallos, J., Bodai, L., Lukacsovich, T., Purcell, J.M., Steffan, J.S., Thompson, L.M., and Marsh, J.L. (2008). Inhibition of specific HDACs and sirtuins suppresses pathogenesis in a Drosophila model of Huntington's disease. Human molecular genetics *17*, 3767-3775.

Petri, S., Korner, S., and Kiaei, M. (2012). Nrf2/ARE Signaling Pathway: Key Mediator in Oxidative Stress and Potential Therapeutic Target in ALS. Neurology research international *2012*, 878030.

Pratt-Hyatt, M., Lickteig, A.J., and Klaassen, C.D. (2013). Tissue distribution, ontogeny, and chemical induction of aldo-keto reductases in mice. Drug metabolism and disposition: the biological fate of chemicals *41*, 1480-1487.

Quintanilla, R.A., and Johnson, G.V. (2009). Role of mitochondrial dysfunction in the pathogenesis of Huntington's disease. Brain research bulletin *80*, 242-247.

Quinti, L., Chopra, V., Rotili, D., Valente, S., Amore, A., Franci, G., Meade, S., Valenza, M., Altucci, L., Maxwell, M.M.*, et al.* (2010). Evaluation of histone deacetylases as drug targets in Huntington's disease models. Study of HDACs in brain tissues from R6/2 and CAG140 knock-in HD mouse models and human patients and in a neuronal HD cell model. PLoS currents *2*.

Rauh, D., Fischer, F., Gertz, M., Lakshminarasimhan, M., Bergbrede, T., Aladini, F., Kambach, C., Becker, C.F., Zerweck, J., Schutkowski, M.*, et al.* (2013). An acetylome peptide microarray reveals specificities and deacetylation substrates for all human sirtuin isoforms. Nature communications *4*, 2327.

Reinhart, P.H., Kaltenbach, L.S., Essrich, C., Dunn, D.E., Eudailey, J.A., DeMarco, C.T., Turmel, G.J., Whaley, J.C., Wood, A., Cho, S.*, et al.* (2011). Identification of anti-inflammatory targets for Huntington's disease using a brain slice-based screening assay. Neurobiology of disease *43*, 248-256.

Reynolds, A.D., Glanzer, J.G., Kadiu, I., Ricardo-Dukelow, M., Chaudhuri, A., Ciborowski, P., Cerny, R., Gelman, B., Thomas, M.P., Mosley, R.L.*, et al.* (2008). Nitrated alpha-synuclein-activated microglial profiling for Parkinson's disease. Journal of neurochemistry *104*, 1504-1525.

Sorolla, M.A., Rodriguez-Colman, M.J., Vall-llaura, N., Tamarit, J., Ros, J., and Cabiscol, E. (2012). Protein oxidation in Huntington disease. BioFactors (Oxford, England) *38*, 173-185.

Stack, C., Ho, D., Wille, E., Calingasan, N.Y., Williams, C., Liby, K., Sporn, M., Dumont, M., and Beal, M.F. (2010). Triterpenoids CDDO-ethyl amide and CDDO-trifluoroethyl amide improve the behavioral phenotype and brain pathology in a transgenic mouse model of Huntington's disease. Free radical biology & medicine *49*, 147-158.

Stack, E.C., Matson, W.R., and Ferrante, R.J. (2008). Evidence of oxidant damage in Huntington's disease: translational strategies using antioxidants. Annals of the New York Academy of Sciences *1147*, 79-92.

Steffan, J.S., Bodai, L., Pallos, J., Poelman, M., McCampbell, A., Apostol, B.L., Kazantsev, A., Schmidt, E., Zhu, Y.Z., Greenwald, M*., et al.* (2001). Histone deacetylase inhibitors arrest polyglutamine-dependent neurodegeneration in Drosophila. Nature *413*, 739-743.

Stepkowski, T.M., and Kruszewski, M.K. (2011). Molecular cross-talk between the NRF2/KEAP1 signaling pathway, autophagy, and apoptosis. Free radical biology & medicine *50*, 1186-1195.

Tieu, K., Ischiropoulos, H., and Przedborski, S. (2003). Nitric oxide and reactive oxygen species in Parkinson's disease. IUBMB life *55*, 329-335.

Tsunemi, T., Ashe, T.D., Morrison, B.E., Soriano, K.R., Au, J., Roque, R.A., Lazarowski, E.R., Damian, V.A., Masliah, E., and La Spada, A.R. (2012). PGC-1alpha rescues Huntington's disease proteotoxicity by preventing oxidative stress and promoting TFEB function. Science translational medicine *4*, 142ra197.

Tsvetkov, A.S., Arrasate, M., Barmada, S., Ando, D.M., Sharma, P., Shaby, B.A., and Finkbeiner, S. (2013). Proteostasis of polyglutamine varies among neurons and predicts neurodegeneration. Nature chemical biology *9*, 586-592.

Tufekci, K.U., Civi Bayin, E., Genc, S., and Genc, K. (2011). The Nrf2/ARE Pathway: A Promising Target to Counteract Mitochondrial Dysfunction in Parkinson's Disease. Parkinson's disease *2011*, 314082.

van Muiswinkel, F.L., and Kuiperij, H.B. (2005). The Nrf2-ARE Signalling pathway: promising drug target to combat oxidative stress in neurodegenerative disorders. Current drug targets *4*, 267-281.

Varma, H., Cheng, R., Voisine, C., Hart, A.C., and Stockwell, B.R. (2007). Inhibitors of metabolism rescue cell death in Huntington's disease models. Proceedings of the National Academy of Sciences of the United States of America *104*, 14525-14530.

Wang, H., Liu, K., Geng, M., Gao, P., Wu, X., Hai, Y., Li, Y., Li, Y., Luo, L., Hayes, J.D.*, et al.* (2013). RXRalpha inhibits the NRF2-ARE signaling pathway through a direct interaction with the Neh7 domain of NRF2. Cancer research *73*, 3097-3108.

Wu, K.C., Cui, J.Y., and Klaassen, C.D. (2012). Effect of graded Nrf2 activation on phase-I and -II drug metabolizing enzymes and transporters in mouse liver. PloS one *7*, e39006.

Xiong, W., MacColl Garfinkel, A.E., Li, Y., Benowitz, L.I., and Cepko, C.L. (2015). NRF2 promotes neuronal survival in neurodegeneration and acute nerve damage. J Clin Invest *125*, 1433-1445.

Yang, B., Fu, J., Zheng, H., Xue, P., Yarborough, K., Woods, C.G., Hou, Y., Zhang, Q., Andersen, M.E., and Pi, J. (2012). Deficiency in the nuclear factor E2-related factor 2 renders pancreatic beta-cells vulnerable to arsenic-induced cell damage. Toxicology and applied pharmacology *264*, 315-323.

Yeager, R.L., Reisman, S.A., Aleksunes, L.M., and Klaassen, C.D. (2009). Introducing the "TCDD-inducible AhR-Nrf2 gene battery". Toxicol Sci *111*, 238-246.

Zadori, D., Klivenyi, P., Szalardy, L., Fulop, F., Toldi, J., and Vecsei, L. (2012). Mitochondrial disturbances, excitotoxicity, neuroinflammation and kynurenines: novel therapeutic strategies for neurodegenerative disorders. J Neurol Sci *322*, 187-191.

Zhang, Y., Talalay, P., Cho, C.G., and Posner, G.H. (1992). A major inducer of anticarcinogenic protective enzymes from broccoli: isolation and elucidation of structure. Proceedings of the National Academy of Sciences of the United States of America *89*, 2399-2403.

Table and Figure Legends

Table 1 Legend. Gene expression analysis of MIND4-treated cells. Statistically significant expression changes of genes for Cases I-III. Genes highlighted in red are upregulated; genes highlighted in green are downregulated. Top seven Canonical Pathways are shown based on significance calculated by IPA for case III (MIND4-treated cells).

Figure 1. Identification potent and selective SIRT2 inhibitor MIND4 . **A, B**) Primary and counter screening of focused library of 8-nitro-5-R-quinoline and 5-nitro-8-R-quinoline derivatives using SIRT2 (**A**) and SIRT3 (**B**) biochemical deacetylation assays. Compounds were screened at single 10 μM concentration in triplicates. Selection of active inhibitors was set at indicated threshold (dotted lines) of <50% of SIRT2 remaining activity; >75% of SIRT3 remaining activity. MIND4 (compound #4) was preliminary identified as a potent selective SIRT2 inhibitor. **C-E**) Concentration-response tests in SIRT1 (**C**), SIRT2 (**D**) and SIRT3 (**E**) biochemical deacetylation assays showed a selective inhibition of SIRT2 by MIND4. **F**) Concentration-response activity test showed no detectable SIRT2 inhibition activity of structural analog MIND4-17. **G**) Structures and SIRT2 inhibition activities of MIND4 analogs. Compound SIRT2 IC_{50}s were established in concentration-response tests *in vitro.*

Figure 2. MIND4 mechanism of SIRT2 inhibition. **A**) Concentration-dependent inhibition of SIRT2 activity by MIND4. **B-C**) Competition of MIND4 with the SIRT2 co-substrate NAD^+ and with acetylated substrate, respectively. Deacetylase activity of SIRT2 was measured at several MIND4 concentrations: 0 μM (empty circles), 0.625 μM (filled circles), 1.2 μM (empty squares), 2.5 μM (filled squares), and 5 μM (triangles). Reactions were conducted at increasing

concentrations of NAD^+ (**B**) or peptide substrate (**C**). The best fitting inhibition model is competitive for NAD^+ and non-competitive for the peptide substrate. **D**) Docking model of the SIRT2/MIND4 complex rationalizes isoform selective inhibition. Overlaid structures of SIRT1 (yellow) (PDB ID 4KXQ), SIRT2 (blue) (3ZGV), and SIRT3 (pink) (4FVT) are presented as cartoons. MIND4, docked in SIRT2, is shown as balls-and-sticks in light blue. Acetylated lysine peptide and non-hydrolyzable NAD^+ analog (carba-NAD^+), shown SIRT3-bound, are presented as pink sticks. The large SIRT2 active site cavity is displayed as a transparent blue surface.

Figure 3. Bioactivity and neuroprotective properties of MIND4. **A-B**) MIND4 treatment increases acetylation of α-tubulin lysine-40 (K40) in wild-type (**A**) and HD mutant (**B**) rat embryonic ST14A cells. Cells were treated with compound for 6 h, then lysates prepared and resolved by SDS-PAGE, and immunoblotted with antibodies specific to acetylated K40 acetylated and total α-tubulin. **C**) Quantification of α-tubulin acetylation from (**A)** and **(B)**. Ratio of acetylated/total α-tubulin in wild-type (black line) and mutant HD (grey lane) was plotted against compound concentration. **E-F**) Effects of MIND4 on increase acetylation of SIRT2 substrates, cytoplasmic α-tubulin and histone 3 (H3), in wild-type primary cortical mouse neurons (DIV 11) treated with compound for 6 h; protein levels analyzed by immunoblotting with respective antibodies. **E**) Effects of MIND4 on acetylation of α-tubulin K40. Total α-tubulin levels were used as loading control. A putative compound target is preferentially expressed as a full-length SIRT2 protein (SIRT2.1 isoform). **F**) Effects of MIND4 on acetylation of H3 lysine-56 (K56), lysine-27 (K27), lysine-9 and lysine-14 (K9/K14). Total H3 levels used as loading control. **G**) MIND4 treatment protects medium spiny neurons (MSNs) in rat *ex vivo* brain slices against toxicity of transiently transfected mutant (73Q) N-terminus HTT fragment (mHTTex1). Yellow fluorescent protein (YFP) was used as a neuronal viability marker and co-transfected with mHTTex1 constructs (black bars). Effects are compared with survival of neurons expressing

YFP plasmid alone (open bar) and expressed as the number of healthy YFP-positive MSNs per brain slice. MIND4 at the indicated concentrations (black bars) and the positive control pan-caspase inhibitor Boc-D-FMK at 100 μM (grey bar) were added directly to the tissue culture media. Statistically significant effect of MIND4 treatment was observed at 10 μM by ANOVA followed by Dunnett's *post hoc* comparison test at the $p<0.05$ confidence level. **H**) MIND4 enhanced survival of photoreceptor neurons in a *Drosophila* model of HD. Relative rescue of photoreceptor neurons, expressing mutant HTTex1 fragment, in flies treated vs. untreated with MIND4 at the10 μM dose was estimated as 22.6%. * = $p <0.001$.

Figure 4. Gene expression profile and IPA analysis. Gene expression profiling and IPA analysis revealed NRF2 as the major pathway impacted by MIND4 in mutant HTT-expressing cells (Case III). **A**) Pathway analysis resulted in lists of IPA "Canonical Pathways," sorted according to Fisher's exact test right-tailed p-value. The top Canonical Pathway was the NRF2-mediated Oxidative Stress Response. This pathway had a highly significant log(p-value) = 13.496. Other pathways are shown in decreasing order of significance to the right. The orange boxes are ratios of the number of MIND4 affected genes in the pathway to the total number in the pathway altogether. **B**) In Case III a fold-change increase of expression of NRF2-responsive genes is shown as a function of color intensity. Large fold-changes are shaded with dark red and decreasing values are shown in lighter red. The pathway shows differential expression in NRF2 downstream targets in mutant HTT expressing cells in the presence and absence of MIND4.

Figure 5. NRF2 activation properties of thiazole analogs MIND4 and MIND4-17. **A-B**) Treatment with MIND4 increased expression of NRF2-responsive proteins NQO1 and GCLM in wild-type (**A**) and in HD mutant (**B**) rat embryonic ST14A cells. Levels of GAPDH were used as loading control. **C**) Treatment with MIND4 increased stability of NRF2. COS1 cells were co-transfected with plasmids encoding NRF2-V5, KEAP1, and β-galactosidase to monitor

transfection efficiencies, and treated for 24 h with MIND4 at 10 μM or the classical NRF2 inducer sulforaphane (SFP) at 5 μM. Cell extracts were prepared, proteins were resolved on SDS-PAGE, and NRF2 levels were detected by immunoblotting with a V5 antibody. **D**) Comparative analysis of NRF2 activation response of NQO1 expression by the SIRT2 inhibitors MIND4 and MIND4-11 in HD mutant ST14A cells. Cells were exposed to compounds for 24 h. Levels of α-tubulin were used as loading control. **E, F**) Treatment with MIND4-17 for 24 h increased expression of the NRF2-responsive proteins NQO1 and GCLM in wild-type (**E**) and in HD mutant (**F**) ST14A cells. Levels of GAPDH used a loading control. **G**) Concentration-dependent induction of the NRF2-responsive proteins NQO1 and GCLM in wild-type mouse cortical neurons (6 DIV) treated with MIND4 or MIND4-17 as indicated for 24 h. Protein expression was detected by immunoblotting. Levels of α-tubulin were used as loading control. **H**) Treatment of primary mouse corticostriatal co-cultures with 5 μM of MIND4-17 induced time-dependent increases in the transcriptional rate of a 5x-ARE promoter-luciferase reporter. *$p<0.05$ by a Student's *t*-test with respect to DMSO-only controls. **I-L)** MIND4-17 induces concentration-dependent increases in transcription of the ARE genes *Nqo1* (**I**), *Hmox1* (**J**) *Gclc* (**K**), and *Srx1* (**L**) as quantified by qPCR. *$p<0.05$ by a Student's *t*-test with respect to DMSO-only controls ("0"). **M, N**) Similar concentration-dependent increases in the transcription of a 5x-ARE-luciferase reporter transfected into wild-type (light grey) vs. mutant HD Q175/+ mouse neurons (black) in corticostriatal co-cultures were induced by treatment with MIND4 (**M**) and MIND4-17 (**N**) for 24 h. *$p<0.05$ by a Student's *t*-test with respect to DMSO-only controls ("0"). **O-P**) Concentration-dependent induction by MIND4 (**O**) and MIND4-17 (**P**) of the NRF2-responsive NQO1 and GCLM proteins in primary mouse astroglia. Cultures were treated for 24 h with MIND4 or MIND4-17 at indicated concentrations. GFAP protein levels were used as the loading control.

Figure 6. NRF2 activating properties of MIND4-17 in microglia cells with intact or knocked down SIRT2 protein. NRF2 activation properties were tested functionally by measuring production of reactive oxygen species (ROS) and reactive nitrogen intermediates (RNI) in LPS/TNFα induced microglia. **A**) N9 microglial cells were lentivirally-transduced with shRNA for SIRT2 knock-down (sh2.1) or with a scrambled control shRNA (shCtr). SIRT2 levels were detected by immunoblotting. **B-C**) ROS levels in stimulated microglia with intact SIRT2 (**B**) or after SIRT2 knockdown (**C**) treated with vehicle (DMSO), MIND4 or MIND4-17. Microglia cells were stimulated with LPS and TNF for 20 h in medium supplemented with compounds at the indicated concentrations. Representative histograms of the fluorescence intensity for the ROS probe showing the overlays of vehicle (DMSO)-treated cells (filled light gray), treated with MIND4 (5 μM) (dotted line) or with MIND4-17 (2.5 μM) (filled dark gray). **D**) RNI production in stimulated microglia cells with functional SIRT2 (white bars) and SIRT2 knockdown (black bars). Cells were treated with vehicle (DMSO), MIND4, and MIND4-17 at the indicated concentrations. RNI was assessed by measurement of iNOS-dependent release of nitrites in the culture supernatants and quantified as percent of control (DMSO-treated cells). Data are presented as mean ± SD of four independent experiments. *$p<0.05$ and **$p<0.01$ by a Student's *t*-test.

Biochemical Pathways	Case I	Case II	Case III
NRF2-mediated Oxidative Stress Response Pathway	*ACTA2 FOSL1 ACTC1 GSTA3 CAT GSTA4 DNAJA1 GSTT2/GSTT2B DNAJB12 JUNB DNAJC15 KRAS DNAJC21 MAF DNAJC14 PRKCH ENC1PRKCZ SOD2*	*ABCC4 HMOX1 ACTA2 JUNB AOX1KEAP1 CAT KRAS DNAJA1 MAFF DNAJA4 MGST1 DNAJC15 MGST2FOSL1 MGST3 GCLC NQO1 GCLM PIK3CD GSR PRKCD GSTA2 PRKCH GSTA3 PRKCZ GSTA4 SOD2 GSTM1 SQSTM1 GSTP1 TXNRD1*	*ABCC4 GSTP1 AOX1 GSTT2/GSTT2B CAT HERPUD1 DNAJA4 HMOX1 DNAJB9 KEAP1 FOSL1 MAFF GCLC MGST1 GCLM MGST2 GSR NQO1 GSTA3 SQSTM1 GSTM5 TXNRD1*
Glutathione-mediated Detoxification	*GGH GSTA3 GSTA4 GSTT2/GSTT2B*	*GSTA2 GSTA3 GSTA4 GSTM1 GSTP1 MGST1 MGST2 MGST3*	*GGH GSTA3 GSTA4 GSTM5 GSTP1 GSTT2/GSTT2B MGST1 MGST2*
LPS/IL-1 mediated inhibition of RXR Function	*ACOX1 GSTA4 ALDH1A2 GSTT2/GSTT2B ALDH1A3 HMGCS1 ALDH1L1 HS3ST1 ALDH1L2 HS3ST6 ALDH3A1 IL33 ALDH6A1 IL1RL1 ALDH9A1 MAOA CAT NGFR CD14 NR1H3 CPT1C PAPSS2 FABP5 RXRA GSTA3 SLC27A3*	*ABCA1 GSTA2 ABCC3 GSTA3 ABCC4 GSTA4 ABCG1 GSTM1 ACOX1 GSTP1 ALAS1 HMGCS1 ALDH1A2 HS3ST1 ALDH1A3 HS3ST6 ALDH1L1 IL1R2 ALDH1L2 MAOA ALDH3A1 MGST1 ALDH9A1 MGST2 CAT MGST3 CD14 NGFR CHST2 NR1H3 CPT1B PAPSS2 CPT1C SLC27A3 FABP5*	*ABCB1 GSTM5 ABCC4 GSTP1 ABCG1 GSTT2/GSTT2B ALAS1 HMGCS1 CAT IL1RL1 CHST2 MAOA CPT1A MGST1 GSTA3 MGST2 SULT1A3/SULT1A4*
Aryl Hydrocarbon Receptor Signaling	*ALDH1A2 HSPB1 ALDH1A3 IL6 ALDH1L1 MYC ALDH1L2 NFIA ALDH3A1 NFIC ALDH6A1 NR2F1 ALDH9A1 RARB CCND1 RARG CYP1A1 RXRA FAS RXRB GSTA3 SRC GSTA4 TGFB2 GSTT2/GSTT2B TGFB3*	*ALDH1A2 GSTM1 ALDH1A3 GSTP1 ALDH1L1 HSPB1 ALDH1L2 IL6 ALDH3A1 MGST1 ALDH9A1 MGST2 APAF1 MGST3 CCND1 NFIA CCND3 NQO1 CYP1A1 NR2F1 CYP1B1 RARB GSTA2 RARG GSTA3 RXRB GSTA4 TGFB3*	*CYP1A1 GSTT2/GSTT2B CYP1B1 IL6 FAS MGST1 GSTA3 MGST2 GSTM5 MYC GSTP1 NFIB NQO1*
Xenobiotic Metabolism Signaling	*ALDH1A2 GSTA4 ALDH1A3 GSTT2/GSTT2B ALDH1L1 HS3ST1 ALDH1L2 HS3ST6 ALDH3A1 IL6 ALDH6A1 KRAS ALDH9A1 MAF CAMK2B MAOA CAT MAP3K3 CITED2 PPP2CB CYP1A1 PPP2R2B GRIP1 PRKCH GSTA3 PRKCZ RXRA*	*ABCC3 HMOX1 ALDH1A2 HS3ST1 ALDH1A3 HS3ST6 ALDH1L1 IL6 ALDH1L2 KEAP1 ALDH3A1 KRAS ALDH9A1 MAOA CAMK2B MGST1 CAT MGST2 CHST2 MGST3 CYP1A1 NQO1 CYP1B1 PIK3CD GCLC PPM1L GRIP1 PPP2CB GSTA2 PPP2R2B GSTA3 PRKCD GSTA4 PRKCH GSTM1 PRKCZ GSTP1 UGT1A1*	*ABCB1 GSTT2/GSTT2B CAT HMOX1 CHST2 IL6 CYP1A1 KEAP1 CYP1B1 MAOA GCLC MGST1 GSTA3 MGST2 GSTM5 NQO1 GSTP1 SULT1A3/SULT1A4*
Glutathione Redox Reactions I		*PX7 GPX8 GPX1 GSR MGST1 MGST2 MGST3*	*GPX1 GSR MGST1 MGST2*
Glutathione Biosynthesis		*GCLC GCLM*	*GCLC GCLM*

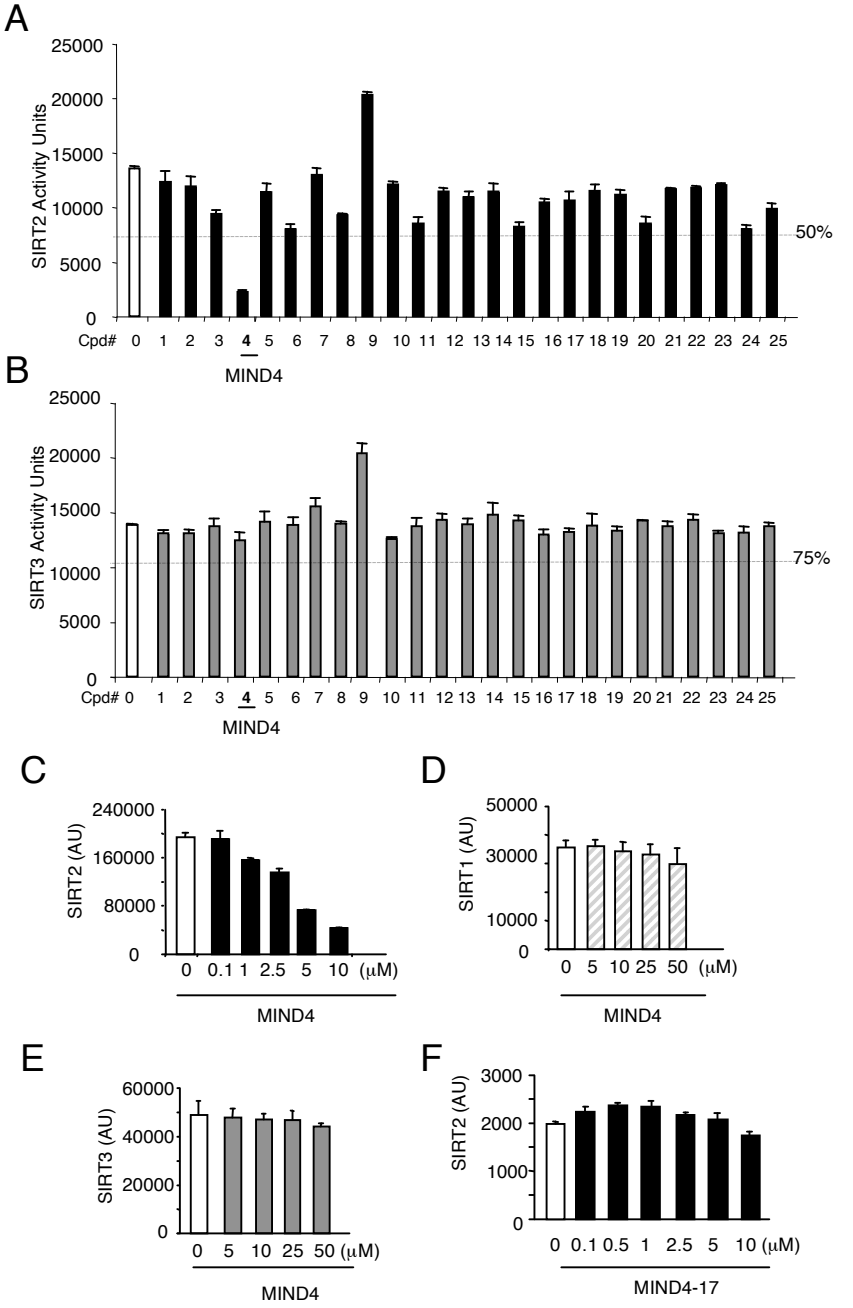
A
SIRT2 Activity Units
25000
20000
15000
10000
5000
0
50%
Cpd# 0 1 2 3 4 5 6 7 8 9 10 11 12 13 14 15 16 17 18 19 20 21 22 23 24 25
MIND4
B
SIRT3 Activity Units
25000
20000
15000
10000
5000
0
75%
Cpd# 0 1 2 3 4 5 6 7 8 9 10 11 12 13 14 15 16 17 18 19 20 21 22 23 24 25
MIND4
C
SIRT2 (AU)
240000
160000
80000
0
0 0.1 1 2.5 5 10 (μM)
MIND4
D
SIRT1 (AU)
50000
30000
10000
0
0 5 10 25 50 (μM)
MIND4
E
SIRT3 (AU)
60000
40000
20000
0
0 5 10 25 50 (μM)
MIND4
F
SIRT2 (AU)
3000
2000
1000
0
0 0.1 0.5 1 2.5 5 10 (μM)
MIND4-17
G
ID MIND4 4A 4-2 4-11 4-12 4-17 4-19 4-20 4-21 4-22 4-23
SIRT2 IC50 3.5 7.5 12 4.0 9.0 >10 7.0 5.0 10 6.0 9.0 (μM)

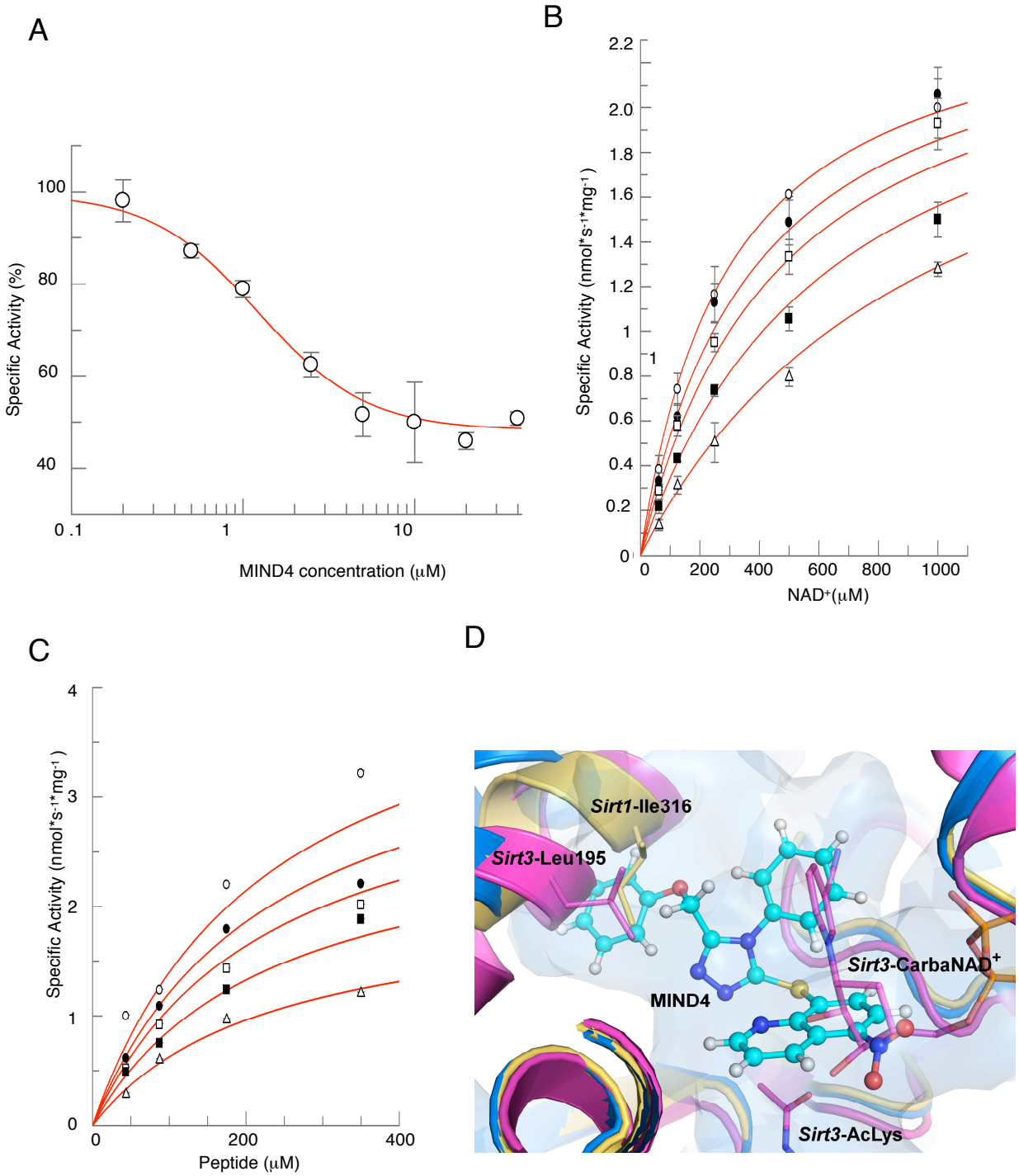
A
Specific Activity (%)
100
80
60
40
0 .1
1
10
MIND4 concentration (μM)
B
Specific Activity (nmol*s-1*mg-1)
2.2
2.0
1.8
1.6
1.4
1.2
1
0.8
0.6
0.4
0.2
0
0
200
400
600
800
1000
NAD+(μM)
C
Specific Activity (nmol*s-1*mg-1)
4
3
2
1
0
0
200
400
Peptide (μM)
D
Sirt1-Ile316
Sirt3-Leu195
Sirt3-CarbaNAD+
MIND4
Sirt3-AcLys

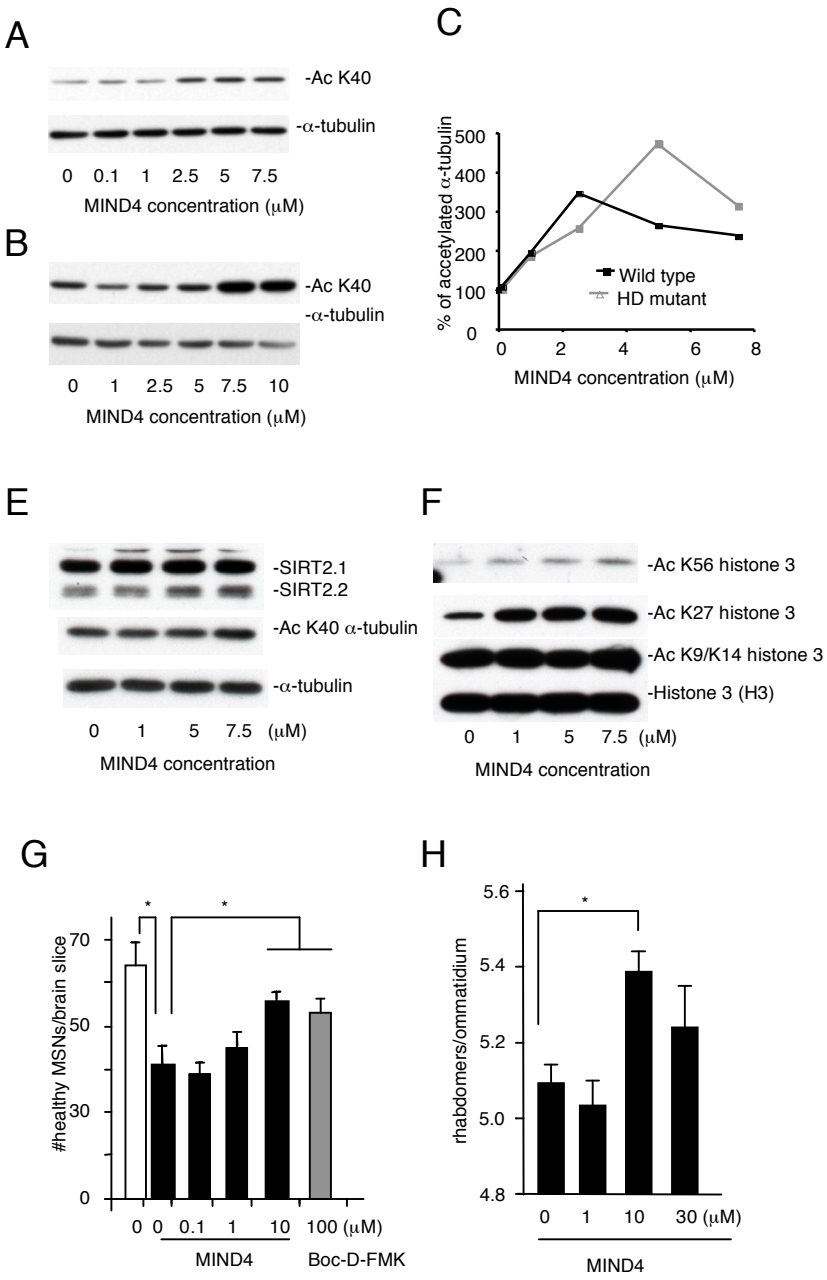
A
-Ac K40
-α-tubulin
0 0.1 1 2.5 5 7.5
MIND4 concentration (μM)
B
-Ac K40
-α-tubulin
0 1 2.5 5 7.5 10
MIND4 concentration (μM)
C
% of accetylated α-tubulin
0 100 200 300 400 500
Wild type
HD mutant
0 2 4 6 8
MIND4 concentration (μM)
E
-SIRT2.1
-SIRT2.2
-Ac K40 α-tubulin
-α-tubulin
0 1 5 7.5 (μM)
MIND4 concentration
F
-Ac K56 histone 3
-Ac K27 histone 3
-Ac K9/K14 histone 3
-Histone 3 (H3)
0 1 5 7.5 (μM)
MIND4 concentration
G
#healthy MSNs/brain slice
0 30 50 70
* *
0 0 0.1 1 10 100 (μM)
MIND4
Boc-D-FMK
H
rhabdomers/ommatidium
4.8 5.0 5.2 5.4 5.6
*
0 1 10 30 (μM)
MIND4

A

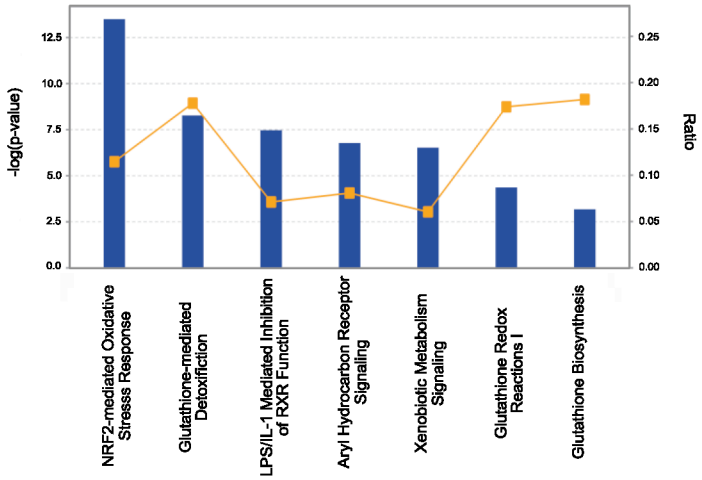
-log(p-value)
Ratio
12.5
10.0
7.5
5.0
2.5
0.0
0.25
0.20
0.15
0.10
0.05
0.00
NRF2-mediated Oxidative Stress Response
Glutathione-mediated Detoxification
LPS/IL-1 Mediated Inhibition of RXR Function
Aryl Hydrocarbon Receptor Signaling
Xenobiotic Metabolism Signaling
Glutathione Redox Reactions I
Glutathione Biosynthesis

B

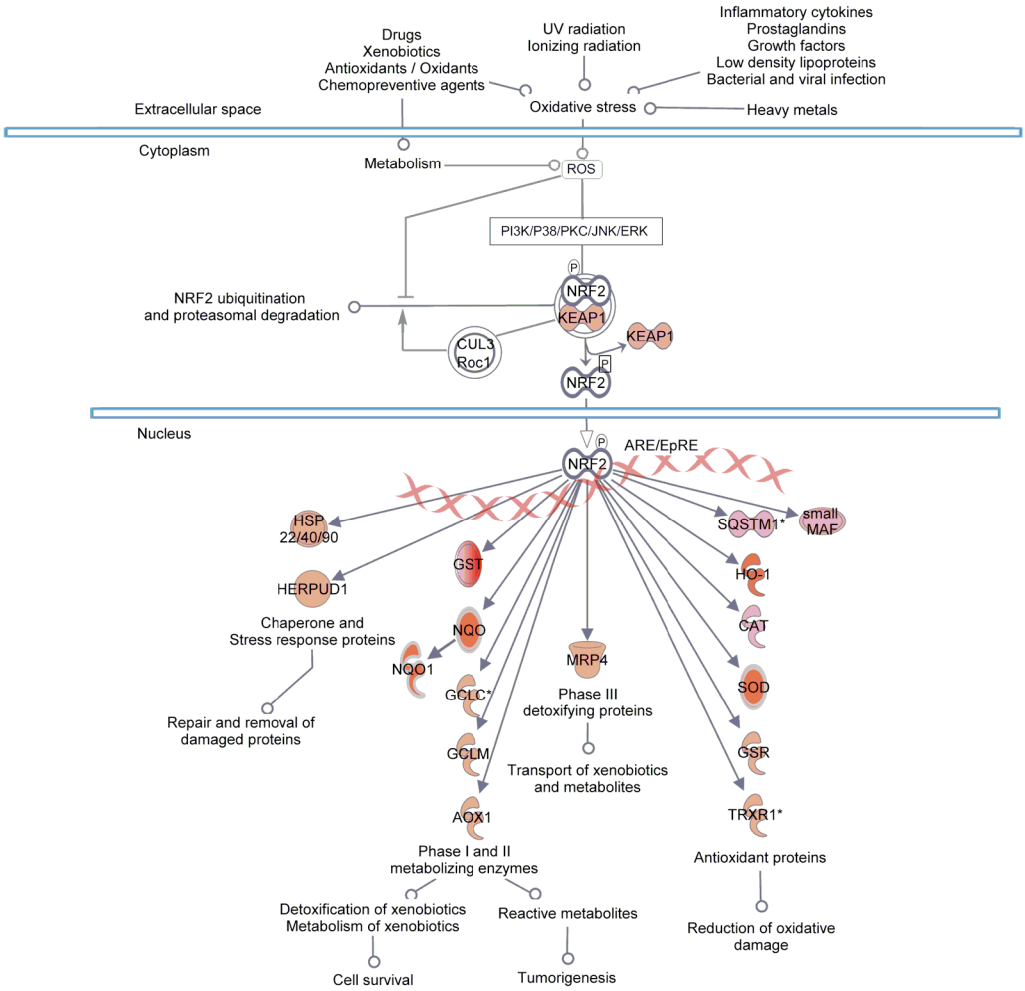
Drugs
Xenobiotics
Antioxidants / Oxidants
Chemopreventive agents
UV radiation
Ionizing radiation
Inflammatory cytokines
Prostaglandins
Growth factors
Low density lipoproteins
Bacterial and viral infection
Extracellular space
Oxidative stress
Heavy metals
Cytoplasm
Metabolism
ROS
PI3K/P38/PKC/JNK/ERK
NRF2 ubiquitination
and proteasomal degradation
NRF2
KEAP1
CUL3
Roc1
Nucleus
ARE/EpRE
HSP
22/40/90
HERPUD1
Chaperone and
Stress response proteins
Repair and removal of
damaged proteins
GST
NQO
NQO1
GCLC*
GCLM
AOX1
Phase I and II
metabolizing enzymes
Detoxification of xenobiotics
Metabolism of xenobiotics
Cell survival
Reactive metabolites
Tumorigenesis
MRP4
Phase III
detoxifying proteins
Transport of xenobiotics
and metabolites
SQSTM1*
small
MAF
HO-1
CAT
SOD
GSR
TRXR1*
Antioxidant proteins
Reduction of oxidative
damage

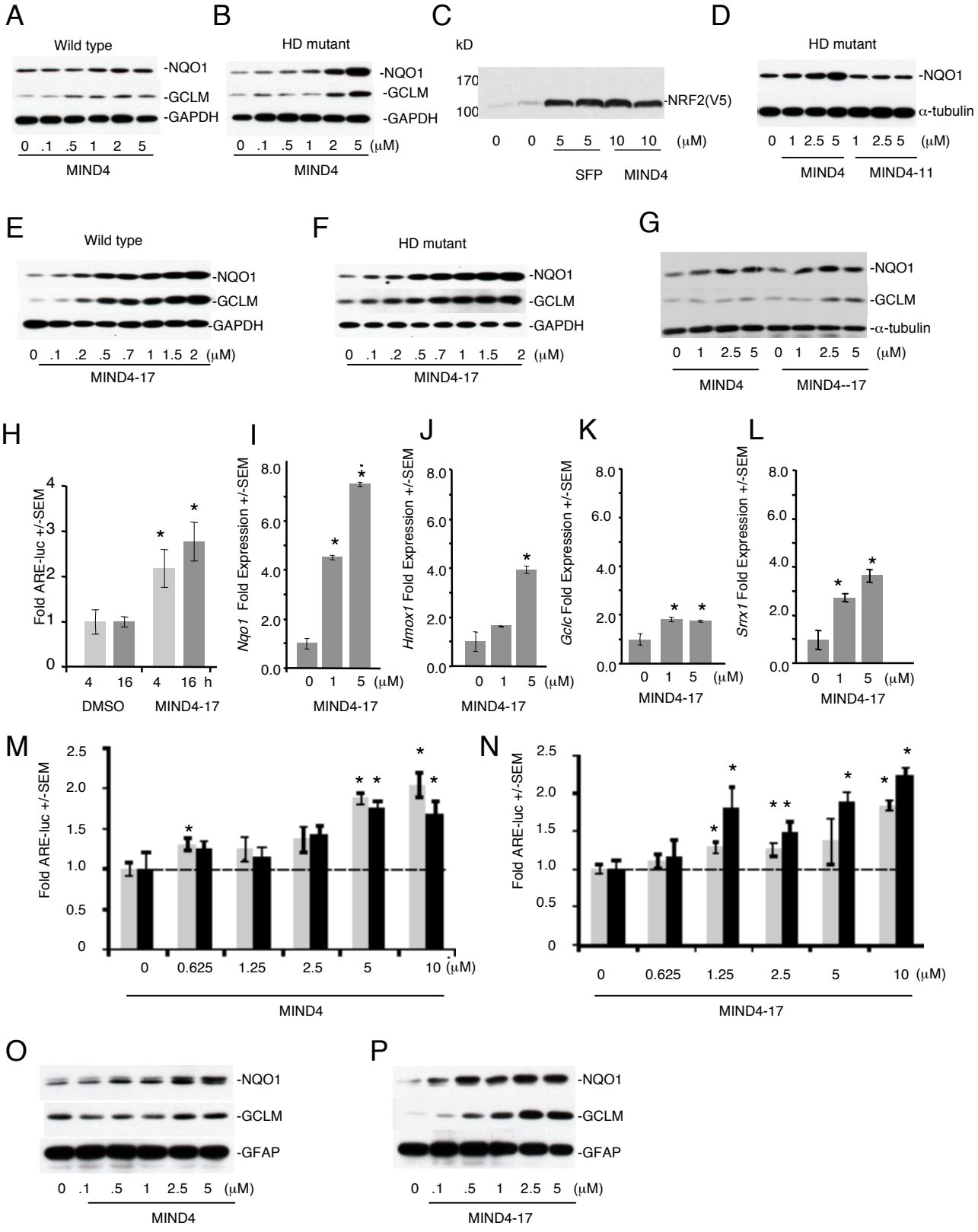
A
Wild type
-NQO1
-GCLM
-GAPDH
0 .1 .5 1 2 5
MIND4
B
HD mutant
-NQO1
-GCLM
-GAPDH
0 .1 .5 1 2 5 (μM)
MIND4
C
kD
170
100
-NRF2(V5)
0 0 5 5 10 10 (μM)
SFP MIND4
D
HD mutant
-NQO1
α-tubulin
0 1 2.5 5 1 2.5 5 (μM)
MIND4 MIND4-11
E
Wild type
-NQO1
-GCLM
-GAPDH
0 .1 .2 .5 .7 1 1.5 2 (μM)
MIND4-17
F
HD mutant
-NQO1
-GCLM
-GAPDH
0 .1 .2 .5 .7 1 1.5 2 (μM)
MIND4-17
G
-NQO1
-GCLM
-α-tubulin
0 1 2.5 5 0 1 2.5 5 (μM)
MIND4 MIND4--17
H
Fold ARE-luc +/-SEM
4 16 4 16 h
DMSO MIND4-17
I
Nqo1 Fold Expression +/-SEM
0 1 5 (μM)
MIND4-17
J
Hmox1 Fold Expression +/-SEM
0 1 5 (μM)
MIND4-17
K
Gclc Fold Expression +/-SEM
0 1 5 (μM)
MIND4-17
L
Srxn1 Fold Expression +/-SEM
0 1 5 (μM)
MIND4-17
M
Fold ARE-luc +/-SEM
0 0.625 1.25 2.5 5 10 (μM)
MIND4
N
Fold ARE-luc +/-SEM
0 0.625 1.25 2.5 5 10 (μM)
MIND4-17
O
-NQO1
-GCLM
-GFAP
0 .1 .5 1 2.5 5 (μM)
MIND4
P
-NQO1
-GCLM
-GFAP
0 .1 .5 1 2.5 5 (μM)
MIND4-17

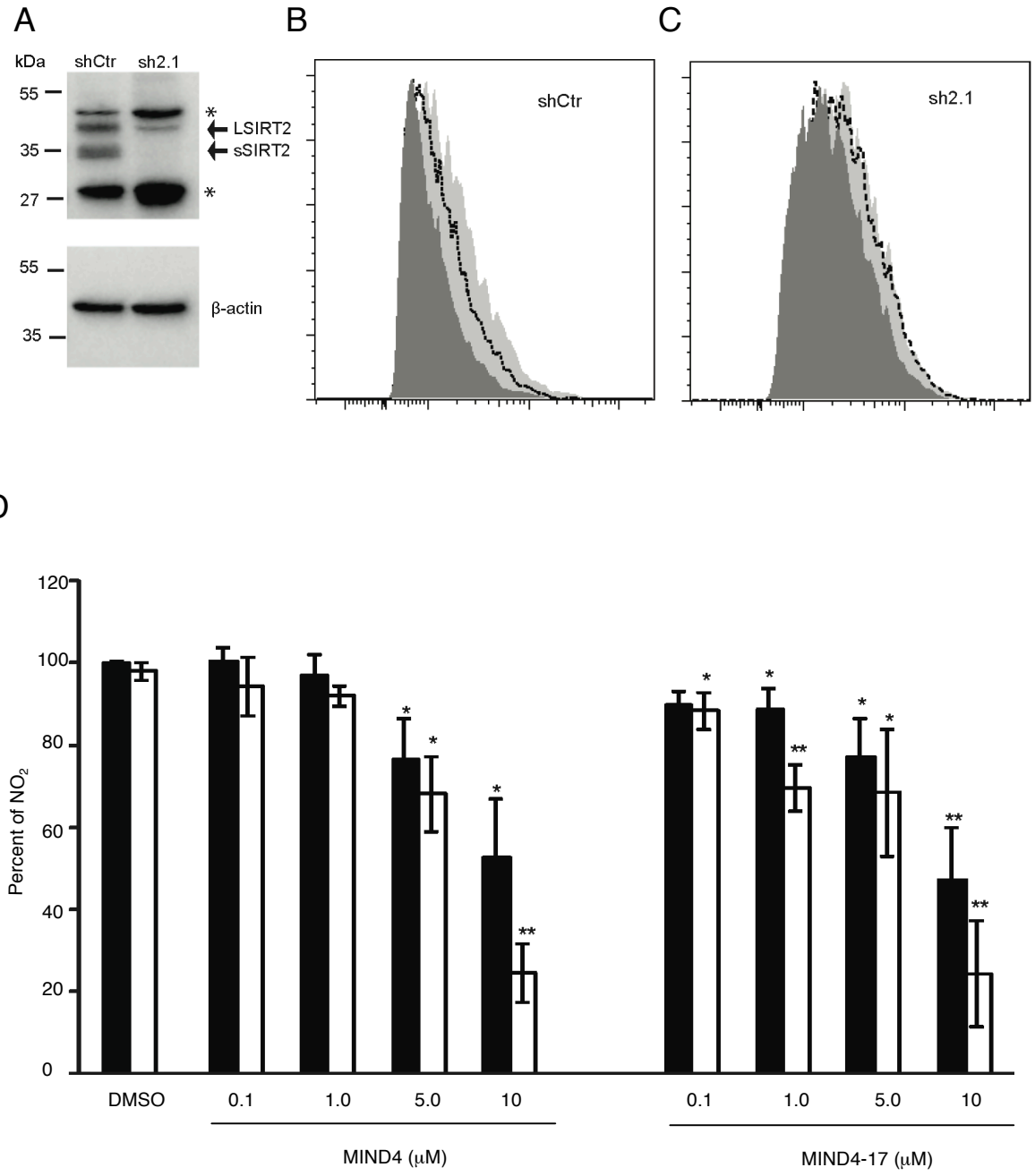
A
B
C
kDa
shCtr
sh2.1
55
35
27
*
LSIRT2
sSIRT2
*
55
35
β-actin
shCtr
sh2.1
D
120
100
80
60
40
20
0
Percent of NO2
DMSO
0.1
1.0
5.0
10
MIND4 (μM)
0.1
1.0
5.0
10
MIND4-17 (μM)

Supplemental Information

Title: A novel structural scaffold of polypharmacological compounds with therapeutic activity in Huntington's disease models

Luisa Quinti [1,*], Malcolm Casale [2,*], Sébastien Moniot [3, *], Teresa F. Pais [4], Michael J. Van Kanegan [5], Linda S. Kaltenbach [5], Judit Pallos [6], Ryan G. Lim [7], Sharadha Dayalan Naidu [8], Heike Runne [9], Lisa Meisel [3], Nazifa Abdul Rauf [1], Dmitriy Leyfer [1], Michele M. Maxwell [1], Eddine Saiah [10], John E. Landers [11], Ruth Luthi-Carter [9], Ruben Abagyan [12], Albena T. Dinkova-Kostova [8, 13], Clemens Steegborn [3], J. Lawrence Marsh [7], Donald C. Lo [5], Leslie M. Thompson [2, 7, 14] and Aleksey G. Kazantsev [1,#]

[*] Author contributed equally

[#] Corresponding author

Inventory

Table S1

Gene	Log Fold Change	P value	FDR Adj P value
GCLC	1.42	2.54E-08	9.99E-07
GCLM	2.32	1.48E-12	2.87E-09
GSTA3	1.31	3.25E-05	0.00057
GSTP1/GSTP2	1.60	2.13E-09	4.60E-07
HERPUD1	1.98	3.98E-11	3.53E-08
HMOX1/HO-1	4.20	1.45E-17	4.51E-13
NQO1	2.03	4.93E-11	3.93E-08
SRX1	2.40	3.90E-15	4.04E-11
SQSTM1	1.25	2.20E-09	4.70E-07
SOD1	0.83	6.65E-05	1.10E-06

Table S1. (Associated with Figure 2). NRF2-responsive genes show increased transcription in wild type rat primary striatal neurons following treatment with 5 μM MIND4 for 24 h.

Fig.S1

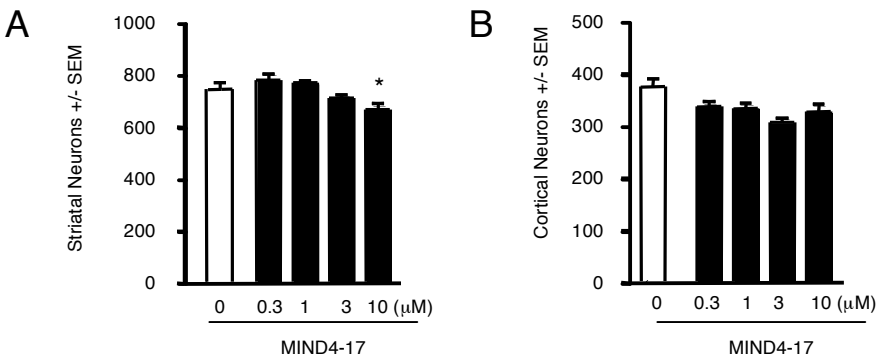
A
Striatal Neurons +/- SEM
1000
800
600
400
200
0
*
0 0.3 1 3 10 (μM)
MIND4-17
B
Cortical Neurons +/- SEM
500
400
300
200
100
0
0 0.3 1 3 10 (μM)
MIND4-17

Fig. S1. (Associated with Figure 5). **A-B**) Treatment with MIND4-17 at indicated tested doses for 24 h is not cytotoxic for primary mouse striatal (**A**) and cortical (**B**) neurons in co culture with astroglia.

Extended Experimental Procedures

Primary striatal rat neuronal cultures

Primary neuronal cultures were prepared from mechanically dissociated ganglionic eminence tissues of wild-type rat embryos embryonic day 16 (E16). This procedure results in a predominant population of Neuronal nuclear antigen (NeuN)-positive and DARPP-32-positive neurons with some astroglia (Runne et al., 2008). Treatments of cultures with MIND4 were at 5 μM, whereas control cultures treated with vehicle (DMSO) only. RNA was extracted by using the RNeasy system (Qiagen), following the manufacturer's protocol. Gene expression changes were assessed by microarray analysis as described previously (Luthi-Carter et al., 2010).

References

Luthi-Carter, R., Taylor, D.M., Pallos, J., Lambert, E., Amore, A., Parker, A., Moffitt, H., Smith, D.L., Runne, H., Gokce, O.*, et al.* (2010). SIRT2 inhibition achieves neuroprotection by decreasing sterol biosynthesis. Proceedings of the National Academy of Sciences of the United States of America *107*, 7927-7932.

Runne, H., Regulier, E., Kuhn, A., Zala, D., Gokce, O., Perrin, V., Sick, B., Aebischer, P., Deglon, N., and Luthi-Carter, R. (2008). Dysregulation of gene expression in primary neuron models of Huntington's disease shows that polyglutamine-related effects on the striatal transcriptome may not be dependent on brain circuitry. J Neurosci *28*, 9723-9731.